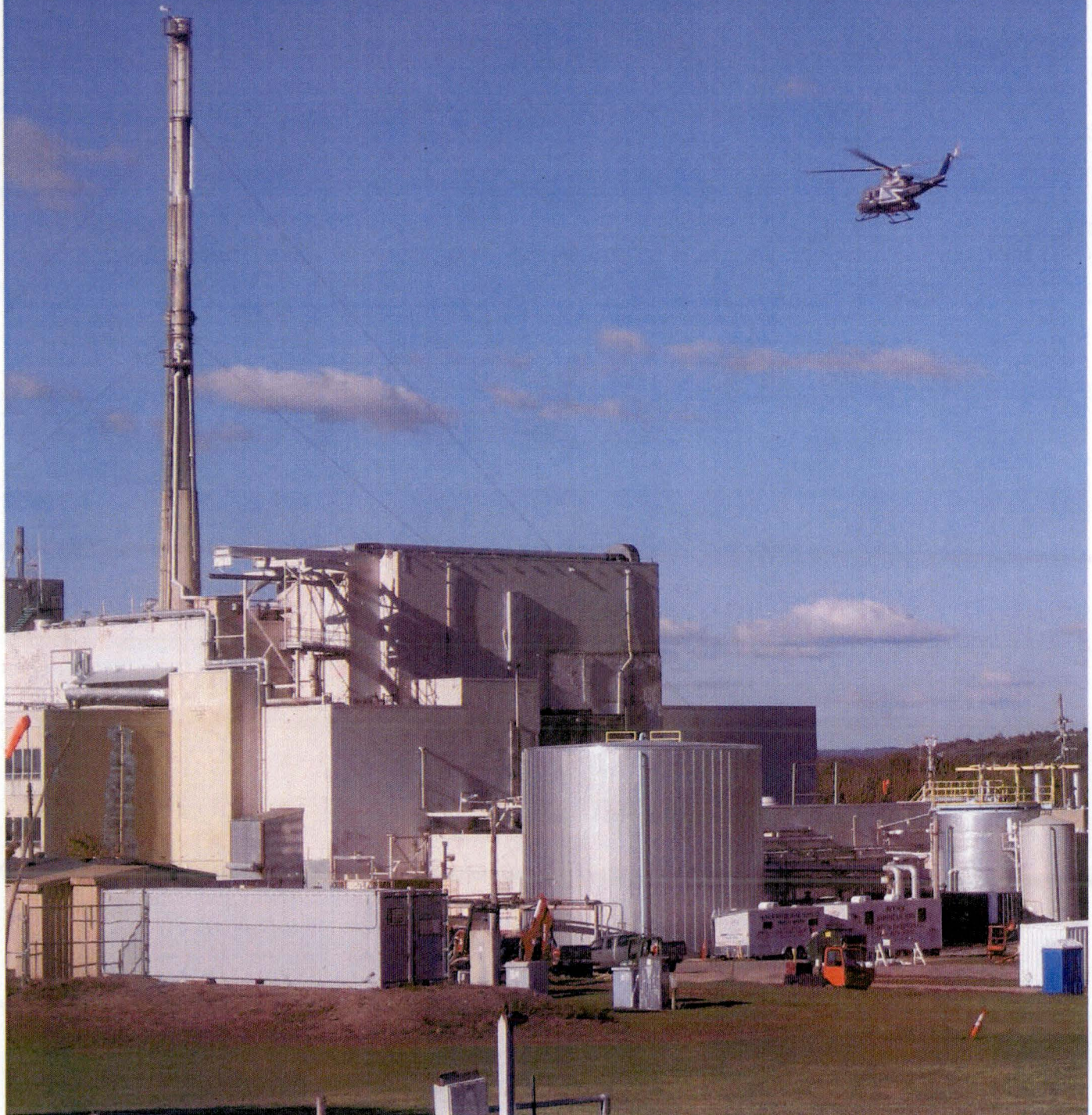


Reference 1 –

An Aerial Radiological Survey of the WNYNSC (RSL. 2015)

# An Aerial Radiological Survey of the Western New York Nuclear Service Center

---



Report date: October 2015

# An Aerial Radiological Survey of the Western New York Nuclear Service Center

---

*Prepared for*

**U.S. Department of Energy (DOE)**

*and*

**New York State**

**Energy Research and Development Authority (NYSERDA)**

Survey dates: September 22 – October 4, 2014

Aerial Measuring Systems

Remote Sensing Laboratory

National Security Technologies, LLC

This document is UNCLASSIFIED



**National Security Technologies LLC**  
*Vision • Service • Partnership*



## DISCLAIMER

This report was prepared as an account of work sponsored by an agency of the U.S. Government. Neither the U.S. Government nor any agency thereof, nor any of their employees, nor any of the contractors, subcontractors or their employees, makes any warranty or representation, express or implied, or assumes any legal liability or responsibility for the accuracy, completeness, or usefulness of any information, apparatus, product, or process disclosed, or represents that its use would not infringe privately owned rights. Reference herein to any specific commercial product, process or service by trade name, trademark, manufacturer, or otherwise, does not necessarily constitute or imply endorsement, recommendation, or favoring by the U.S. Government or any agency thereof. The views and opinions of authors expressed herein do not necessarily state or reflect those of the U.S. Government or any agency thereof.

## **Executive Summary**

At the request of the U.S. Department of Energy (DOE) and the New York State Energy Research and Development Authority (NYSERDA), the National Nuclear Security Administration's Remote Sensing Laboratory conducted an aerial radiological survey over the Western New York Nuclear Service Center (WNYNSC) and Cattaraugus Creek in western New York State. The WNYNSC is owned by NYSERDA and is the site of a former commercial nuclear fuel reprocessing facility that is now part of an environmental cleanup managed by the DOE as part of the West Valley Demonstration Project (WVDP). The goal of the survey was to provide an updated picture of radiological conditions at the WNYNSC in relation to previous surveys performed in 1979 and 1984, and to extend the area coverage relative to these surveys to assess conditions along the Cattaraugus Creek flood plains downstream of the WNYNSC.

An aggregate area of approximately 90 square miles was surveyed over the course of nineteen flights in eleven days between September 22 and October 2, 2014. A total of 31 ground-based exposure rate measurements were taken to validate the method of inferring exposure rate on the ground from count rate data collected at survey altitude. Interpolative contour maps were produced from the aerial spectral data to show inferred exposure rates at one meter above ground due to terrestrial sources (that is, excluding contributions from cosmic rays and airborne radon and radon daughter products), relative levels of radiation due to anthropogenic (man-made) sources, and relative levels of radiation from two specific radioisotopes known to be present: cobalt-60 and cesium-137.

In general, patterns of radiation levels at and near the WNYNSC are consistent with those observed in previous surveys. Localized cobalt-60 signatures observed within the WVDP boundaries are consistent with the presence of radioactive waste storage facilities on the site. The overall footprint of elevated exposure rates observed on the WVDP site in 1984 appears to have shifted in the 2014 data. Levels of cesium-137 contamination have weakened along the so-called "cesium prong" extending northwest from the site and also along Buttermilk Creek as compared to the 1984 survey results, likely due to a combination of dilution and dispersion in the environment and radioactive decay.

Previous surveys identified areas outside the WNYNSC with radiation levels slightly above background. Background radiation includes naturally occurring radiation sources as well as some man-made sources (such as radiation in the environment as a result of atomic testing). The 2014 survey also identified certain new areas outside the WNYNSC with above-background radiation levels. The aerial radiation measurements for these areas are only slightly elevated above observed background radiation levels. While the aerial survey does not directly measure potential contaminant concentrations in soil, the results presented herein can be used to inform further, more focused direct measurements where warranted.

## **Table of Contents**

Executive Summary.....	vii
List of Figures .....	x
List of Tables .....	x
Acronyms .....	xi
1 Introduction .....	1
2 Survey Area .....	1
3 Survey Operations.....	2
3.1 Data Acquisition Equipment .....	2
3.2 Conduct of Aerial Measurements .....	5
3.3 Conduct of Ground-Based Measurements .....	8
4 Data Analysis.....	8
4.1 Gross Count Rate Analysis and Conversion to Terrestrial Exposure Rate .....	9
4.2 Analysis of Anthropogenic Sources.....	12
4.3 Isotopic Extractions.....	13
5 Survey Results .....	15
5.1 Fixed Ground Measurements .....	15
5.1.1 Test Line and Altitude Spiral .....	18
5.1.2 Site Interior .....	18
5.1.3 Flood Plain.....	20
5.2 Exposure Rate Maps .....	20
5.3 Anthropogenic Extractions.....	24
5.4 Isotopic Extractions.....	28
5.4.1 Cesium-137 .....	28
5.4.2 Cobalt-60.....	32
5.4.3 Technetium-99m.....	32
5.5 Comparison to Previous Surveys.....	33
5.5.1 Representative Exposure Rates from Selected Areas.....	33
5.5.2 Comparison of Current Results to 1984 Survey.....	34
References .....	37
Survey Parameters .....	38

## List of Figures

Figure 1: Survey area .....	2
Figure 2: RSX-3 detector unit .....	3
Figure 3: Components of the RSI data acquisition system .....	3
Figure 4: AMS Bell 412 helicopter with externally mounted detector pods .....	4
Figure 5: Gamma in situ measurement instruments .....	5
Figure 6: Radiation survey flight schematic .....	6
Figure 7: Typical spectrum of natural radioactive background .....	9
Figure 8: Example fit of altitude spiral flight data.....	10
Figure 9: Average count rates from water and test lines .....	11
Figure 10: Three-window cesium-137 extraction from spectra .....	14
Figure 11: Exposure rate measurements taken with the PIC around WNYNSC .....	16
Figure 12: Exposure rate measurement taken with the PIC near Zoar Valley.....	17
Figure 13: Comparison of exposure rates from AMS and PIC measurements .....	19
Figure 14: Exposure rates at 1 m above ground due to terrestrial sources (full survey area) .....	22
Figure 15: Exposure rates at 1 m above ground due to terrestrial sources (detail over WNYNSC) .....	23
Figure 16: Anthropogenic extraction map (full survey area).....	25
Figure 17: Anthropogenic extraction map (detail over WNYNSC).....	26
Figure 18: Cesium-137 spectral signature from Flood Plain 3 .....	27
Figure 19: Cesium-137 isotopic extraction map (full survey area) .....	29
Figure 20: Cesium-137 isotopic extraction map (detail over WNYNSC) .....	30
Figure 21: Cesium-137 isotopic extraction map (detail over western Cattaraugus Creek).....	31
Figure 22: Cobalt-60 isotopic extraction map (detail over WNYNSC) .....	32
Figure 23: Technetium-99m spectral signature from Thomas Indian School Drive .....	33
Figure 24: Comparison of the 2014 survey to the 1984 survey.....	36

## List of Tables

Table 1: Comparison of average exposure rates for test line, altitude spiral, and WVDP site exterior .....	18
Table 2: Exposure rate at various areas of interest from surveys between 1968 and present.....	34

## **Acronyms**

ADS	Advanced Digital Spectrometer
AGL	above ground level
AMS	Aerial Measuring System
AVID	Advanced Visualization and Integration of Data
DOE	U. S. Department of Energy
GPS	Global Positioning System
HPGe	high-purity germanium
NYSERDA	New York State Energy Research and Development Authority
PIC	pressurized ionization chamber
RSI	Radiation Solutions, Inc.
RSL	Remote Sensing Laboratory
WNYNSC	Western New York Nuclear Service Center
WVDP	West Valley Demonstration Project

## **1 Introduction**

The Western New York Nuclear Service Center (WNYNSC), owned by the New York State Energy Research and Development Authority (NYSERDA), is a 3,300-acre site in western New York located approximately 30 miles south of Buffalo. Located at the WNYNSC is a former commercial nuclear fuel reprocessing facility being decommissioned by the West Valley Demonstration Project (WVDP), managed by the U.S. Department of Energy (DOE) (USDOE/NYSERDA 2010).

At the request of DOE and NYSERDA, an aerial radiological survey was conducted over the WNYNSC and along Cattaraugus Creek west to Lake Erie by an Aerial Measuring System (AMS) team from the National Nuclear Security Administration's Remote Sensing Laboratory (RSL). The RSL is managed and operated by National Security Technologies, LLC, at Nellis Air Force Base in Las Vegas, Nevada, and Joint Base Andrews in Suitland, Maryland. The goal of the survey was to provide an updated picture of radiological conditions at the WNYNSC in comparison to a similar survey conducted in 1984 (EG&G/EM 1991), and to extend the area coverage relative to previous surveys to assess conditions along the Cattaraugus Creek flood plains between the WNYNSC and Lake Erie. Earlier surveys of the area were performed in 1979 (EG&G/EM 1981) and annually between 1968 and 1970 during the operation of the nuclear fuel reprocessing facility (Barasch and Beers 1971).

The survey was conducted from September 22 through October 2, 2014. An aggregate area of approximately 90 square miles was surveyed over the course of nineteen flights in eleven days. A total of 31 "ground truth" exposure rate measurements were taken at selected fixed locations on the ground as a consistency check on the method used to convert count rates in the aerial detectors to exposure rates on the ground. Interpolative contour maps were produced from the aerial spectral data to show inferred exposure rates at one meter above ground due to terrestrial sources, extracted count rates from low-energy radiation corresponding to anthropogenic sources, and extracted count rates from two specific radioisotopes known to be present: cesium-137 and, on the WVDP site only, cobalt-60.

## **2 Survey Area**

As requested by DOE and NYSERDA, the survey area was chosen not only to include the area over the WNYNSC that had previously been studied in 1984, but also to extend to the Cattaraugus Creek flood plains leading west from the WNYNSC out to Lake Erie. This area includes portions of New York's Cattaraugus, Chautauqua and Erie Counties, as well as parts of the Cattaraugus Territory of the Seneca Nation of Indians. All measurements, both aerial and ground-based, were taken in coordination with appropriate local, state, and DOE officials, and the general survey plan was presented by DOE, NYSERDA and AMS at a West Valley, New York public meeting in August, 2014.

The survey area was divided into six distinct "boxes" for operational reasons (Figure 1). Aerial surveys are typically flown in a series of parallel lines over the survey area such that the effective field of view of the detectors sweeps over the entire area (see Survey Operations below). Visual feedback from a global positioning system (GPS) navigation device aids the pilots in maintaining a straight flight path. Given the meandering path of Cattaraugus Creek, it was much simpler operationally to divide the survey area into

a series of boxes that enclose the flood plains and allow for straight-line flying while excluding (to the extent practical) areas outside the requested survey area. This approach minimizes flight time and allows the pilots to take advantage of the GPS feedback for steering.

As seen in Figure 1, the survey box covering the WNYNSC (in yellow) and the immediately downstream section of Cattaraugus Creek is labeled "West Valley" in the legend. Buttermilk Creek, which carries surface water from the WVDP site through the WNYNSC to Cattaraugus Creek, also falls within the West Valley survey box. The remaining five boxes are labeled "Flood Plain 1" through "Flood Plain 5."

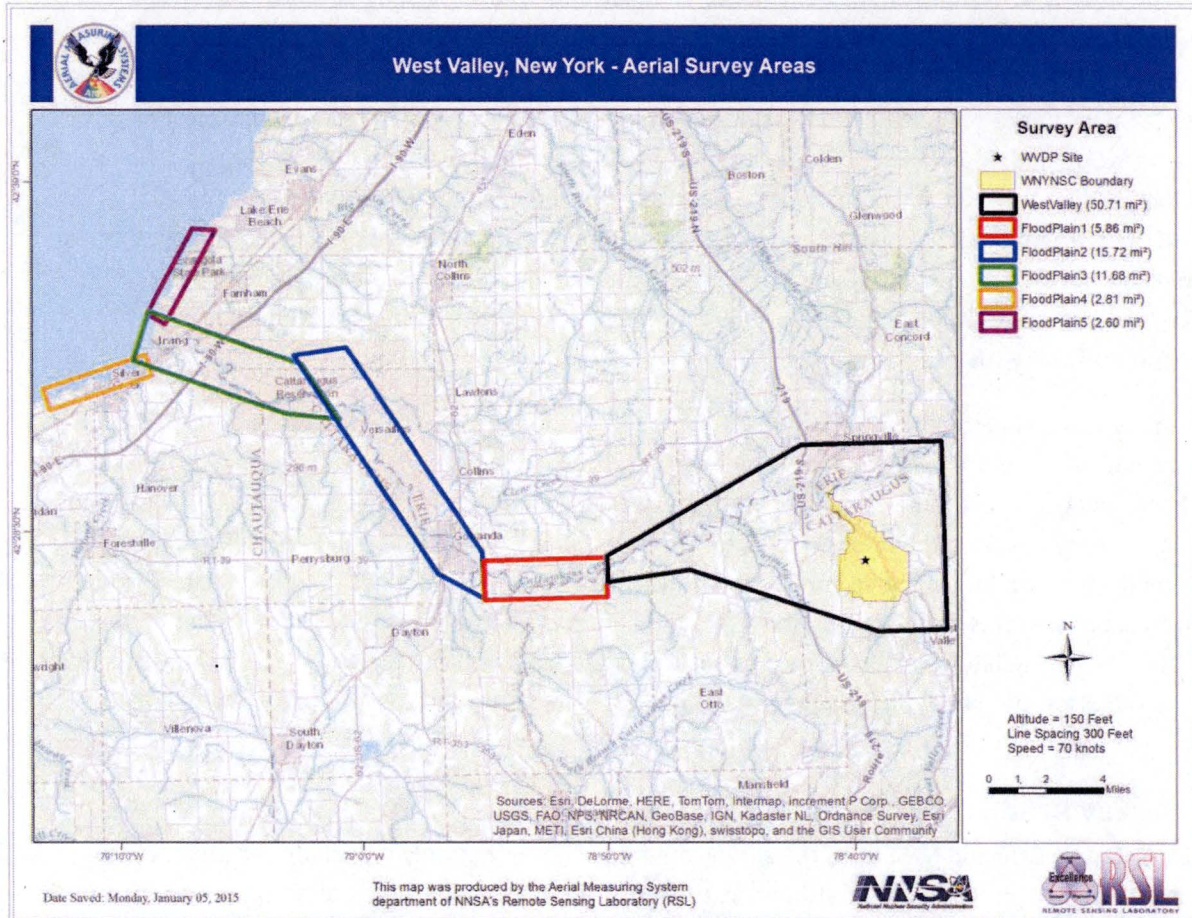


Figure 1: Survey area, comprised of six survey boxes.

### 3 Survey Operations

#### 3.1 Data Acquisition Equipment

AMS uses a gamma-ray detection system developed by Radiation Solutions, Inc. (RSI), for acquisition of aerial survey data. The RSI system employs a total of twelve thallium-activated sodium iodide (NaI(Tl)) scintillator crystals with dimensions 2" x 4" x 16" (approximately 2 liters volume per crystal). The detectors are packaged in four RSX-3 units, each of which contains three NaI(Tl) scintillators coupled to

photomultiplier tubes which in turn produce analog signals for multichannel digital processing by Advanced Digital Spectrometer (ADS) modules (Figure 2).

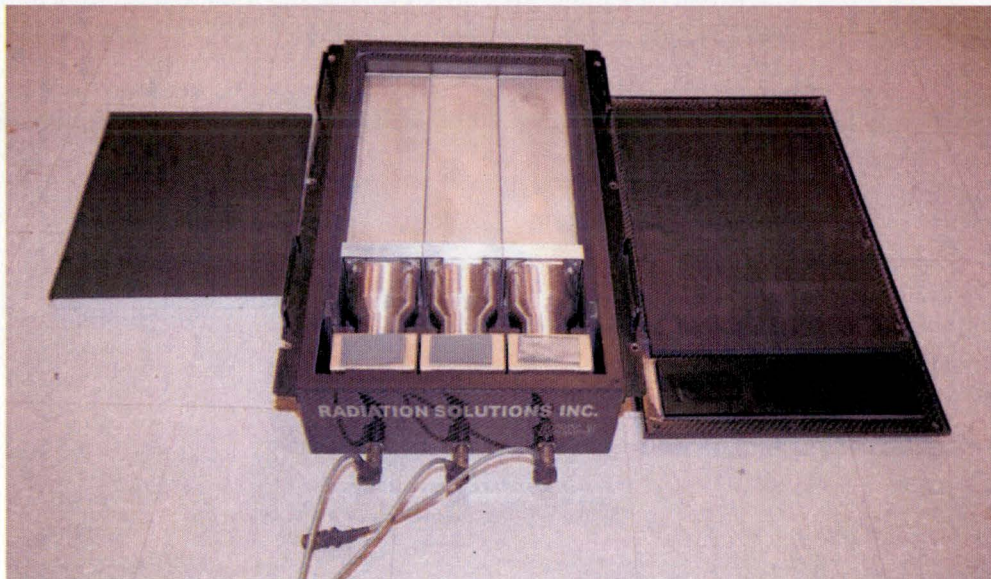


Figure 2: RSX-3 detector unit with three 2" × 4" × 16" NaI(Tl) scintillators, three photomultiplier tubes, and three ADS modules.

Once per second, gamma-spectral data from each of the three ADS modules are sent to an RS-701 console which manages each detector's data stream and is able to dynamically adjust detector gain to compensate for spectral drift. The digital output from the four RSX-3/RS-701 units is aggregated by an RS-501 console which stores the data and allows it to be monitored real-time in the aircraft via an Ethernet connection to a laptop computer (Figure 3). The RS-501 unit also provides power distribution and houses the Trimble differential GPS receiver. The laptop computer controls the configuration, startup and shutdown of the data acquisition system using RSI's RadAssist software via the RS-501.



Figure 3: Components of the RSI data acquisition system.

The RSI data acquisition system is mounted and flown on a Bell 412 twin-engine helicopter capable of approximately 2.5 hours of continuous flight time between refueling, as loaded and configured for survey operations. The RSX-3/RS-701 units are fitted into two aluminum pods mounted external to the helicopter (Figure 4), with two RSX-3/RS-701 units in each pod.



Figure 4: AMS Bell 412 helicopter with externally mounted detector pods.

The primary function of the Trimble GPS antenna and receiver is to record the geolocation of the helicopter as a critical component of the survey data. However, the GPS signal is also used in conjunction with a second receiver mounted in the aircraft cabin for steering assistance. The desired flight path is loaded into the GPS receiver and continuously compared to the aircraft location, such that any deviation from the flight path is communicated to a heads-up LED display mounted in the peripheral vision of the pilots. This visual feedback assists the pilots in maintaining a straight flight path and ultimately improves the quality of data interpolation during analysis.

While the RSI RadAssist software is employed on the aircraft cabin laptop to configure and control the RSI system, the equipment technologist also uses software developed by RSL, Advanced Visualization and Integration of Data (AVID), to monitor the incoming spectral data, perform in-flight checks of data quality, and watch for anomalies in the data using configurable count-rate or spectral alarm metrics. AVID is also capable of transmitting the second-by-second spectral data over a cellular or satellite connection to a ground-based server, which can then be monitored in near real time by a data analyst connected to the same server. In-flight data telemetry is useful for streamlining data post-processing tasks, but it is not necessary as the data are always stored locally on both the aircraft cabin laptop and on the RS-501 unit.

Measurements of exposure rate on the ground and high-resolution gamma spectra from terrestrial sources are taken in support of the aerial measurements to corroborate the terrestrial exposure rate

(Section 4.1) and isotopic extraction (Section 4.3) analyses. These in situ measurements are performed using a GE Reuter-Stokes 131 pressurized ionization chamber (PIC) to measure exposure rate and an ORTEC Detective-EX mechanically cooled high-purity germanium (HPGe) gamma-ray spectrometer, each mounted on a tripod at one meter above ground as shown in Figure 5. The face of the HPGe spectrometer is pointed at the ground to optimally detect gamma rays from terrestrial sources. A tripod-mounted Trimble GPS antenna and receiver are used to geolocate each ground measurement.



Figure 5: Gamma in situ measurement using ionization chamber, GPS antenna, and high-purity germanium spectrometer.

### **3.2 Conduct of Aerial Measurements**

The AMS team based its operations for this survey at the Prior Aviation fixed base operator at Buffalo Niagara International Airport in Cheektowaga, NY. This location provided access to secure equipment storage and office space, aircraft parking and fuel, proximity to Lake Erie for water line measurements (described below), and a reasonable transit time to and from survey areas that were geographically extensive.

The minimum AMS crew on each survey flight consisted of two pilots to fly the survey pattern and an equipment technologist to monitor data acquisition. Occasionally, the mission manager or a data scientist would also fly to monitor data quality and decide if in-flight modifications to the mission plan were needed. During this survey, four non-RSL personnel from three agencies with stakeholder interest in the survey – DOE, NYSERDA, and New York State Department of Environmental Conservation – participated in some flights as qualified non-crew members to help them understand the data acquisition process and better interpret the analyses presented in this report.

Three times during the course of this survey, a predetermined line over land was flown at multiple altitudes to empirically determine the air attenuation coefficient for terrestrial radiation. This line is called an "altitude spiral," and for this survey it was flown at 100, 200, 300, 500, and 900 feet above ground level (AGL) in an area approximately two miles north of the WVDP site where the geography and radiological signature are both relatively flat. The altitude spiral measurements allow for the conversion of count rates in the detectors to an inferred exposure rate on the ground from terrestrial sources (see Section 4, Data Analysis).

The survey was flown in a back-and-forth serpentine pattern of successive straight lines, with spacing between adjacent lines equal to twice the nominal altitude above ground level (Figure 6). A line spacing of twice the altitude is usually chosen to achieve full coverage of the survey area because the effective field of view of the aircraft-mounted detectors is nominally a circle on the ground with a diameter of approximately twice the aircraft altitude (Proctor 1997).

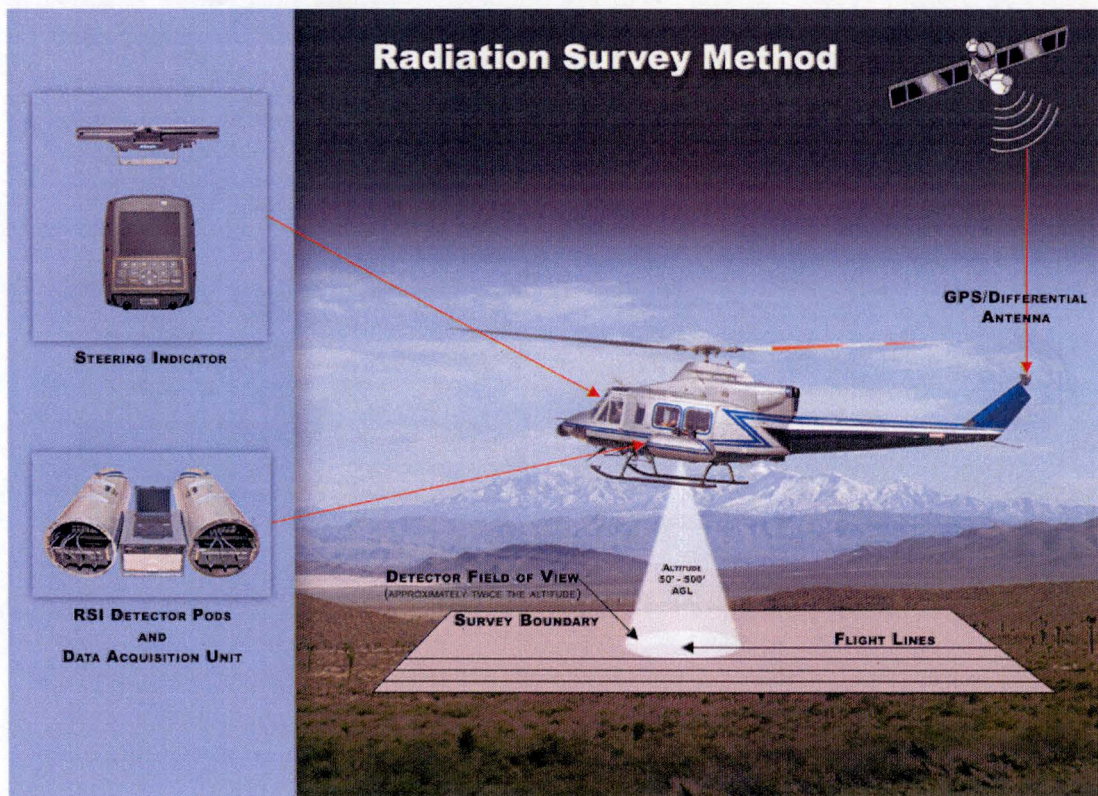


Figure 6: Radiation survey flight schematic. Because the diameter of the circular area effectively seen by the detectors is twice the helicopter's altitude, adjacent parallel lines are flown at a spacing of twice the altitude (one diameter) for complete coverage.

Flight line headings are chosen by considering geographic constraints and the general shape of the survey box. The West Valley box (Figure 1) was flown with north-south line headings due to glacially carved valleys running north to south in that area; it was easier for the pilots to maintain a constant altitude above ground by following the valleys. The Flood Plain boxes were flown with headings parallel to the long edge of each box; with no significant terrain constraints, the most efficient way to cover a rectangular box is by flying parallel to the long edges, minimizing the time and fuel spent on turns. As

configured and loaded for this survey, the Bell 412 helicopter's fuel capacity restricted each flight to approximately two and a half hours of flight time. When multiple flights were needed to cover one box, each successive flight would repeat the last line flown on the previous flight as a consistency check and to allow for data corrections if needed.

Each day that survey flights were performed, the acquisition system and the data collected were subjected to multiple operational and quality checks. Prior to each day's flights, the proper calibration, operation, and detector response of the RSI system were verified on the ground using natural terrestrial background and small (approximately 7  $\mu\text{Ci}$ ) cesium-137 check sources. The integrity of the GPS and altimeter signals was also verified each morning prior to launch.

Several times each day, at the beginning or at the end of each survey flight (or sometimes both), a line was flown at nominal survey altitude and speed over Lake Erie, called a "water line." At a sufficient water depth and distance from the shore, the water effectively shields all contributions to the gamma ray count rate in the detectors from terrestrial sources, but does not shield radiation from any airborne radon or radon daughters, or background from cosmic rays. Measurement on the water line thus allows for the extraction of count rates due only to terrestrial sources (see Section 4, Data Analysis). The water line was flown several times over the course of each survey day to monitor the effect of diurnal and other variations in atmospheric radon concentration and correct the data from each survey flight accordingly.

At the beginning and end of each survey flight, a line was flown at nominal survey altitude and speed over a predetermined strip of land, called a "test line." The test line for this survey was a one-mile strip of rural road near North Collins, New York, surrounded by relatively homogeneous, level terrain on either side. Data collected over the test line were examined for consistency from one flight to the next, such that any deviations to the count rate outside of expected statistical and radon-related fluctuations could be examined for evidence of equipment malfunction. No such deviations along the test line were observed during this survey.

At the conclusion of each survey flight, data were retrieved from the aircraft cabin laptop and assessed for quality by a data scientist. Detector count rates, spectral shapes, flight paths, GPS continuity, altimeter readings, and any water line and test line data were reviewed for consistency. If any inconsistencies or abnormalities were discovered, the data were flagged for potential re-collection if necessary, and further survey flights were held until the cause of the inconsistency could be understood and any problems corrected. This occurred once during the conduct of the survey, when the post-flight check of data quality revealed that an individual detector from one of the RSX-3/RS-701 units had dropped from the data stream mid-flight. The malfunctioning detector was investigated and the problem was corrected prior to the next flight, and the survey area over which the detector had malfunctioned was re-flown during a later flight.

This survey was flown at a ground speed of 70 knots (36 meters per second), at a nominal altitude of 150 feet (46 meters) AGL with a spacing of 300 feet (91 meters) between lines. In general, practical considerations make it impossible for the pilots to precisely maintain the nominal survey altitude above

ground. To compensate, the radar altimeter signal is captured in the data stream and used to correct the radiation data to the nominal survey altitude (see Section 4, Data Analysis).

The total survey area (including all altitude spirals, test lines and water lines) was covered in a total of nineteen flights conducted over ten days between September 22 and October 1, 2014.

### **3.3 Conduct of Ground-Based Measurements**

As a verification of the method used to convert gamma-ray count rates to exposure rates at one meter above ground, a series of measurements were taken on the ground within the survey area and along the test line and altitude spiral using the Reuter-Stokes PIC and Detective-EX HPGe spectrometer. The PIC records an exposure rate due to all components of the background: terrestrial sources, airborne radon and daughters, and cosmic rays; therefore, when comparing to exposure rate due to terrestrial sources inferred from the aerial data, the radon and cosmic-ray contributions must be accounted for. From the HPGe spectra, with some knowledge about the distribution of radioisotopes on or in the soil, approximate concentrations of contaminant isotopes could be calculated. For this survey, however, HPGe spectra were collected primarily to investigate whether contaminant isotopes were present, in support of the aerial and PIC measurements.

## **4 Data Analysis**

AMS records once-per-second 1024-channel gamma-ray spectral events tagged with radar altimeter reading and GPS location. The spectral channels are summed to generate aggregate count rate data, and analysis is done to convert the count rate data to an exposure rate at one meter above ground due to terrestrial sources. From the spectral data, algorithms that employ appropriate spectral windows are applied to infer relative levels of anthropogenic sources versus naturally occurring background and to extract relative levels of specific radioisotopes expected to be present. A typical background spectrum is shown in Figure 7; the annotated peaks are signatures of specific naturally occurring radioisotopes.

Because the GPS time stamp on each data event occurs at the beginning of the sampling interval, each data point must be time-shifted forward by one half-second to correctly correspond to the center of the effective sampled area beneath the aircraft. At the nominal survey ground speed of 70 knots, this corresponds to a measurement offset of 60 feet. The time-corrected pointwise exposure rate and extracted count rate data can then be interpolated using an inverse-distance-weighting method to generate continuous contoured data in geographic information system format. Without this time correction, the contoured data would exhibit sawtooth-like artifacts when mapped.

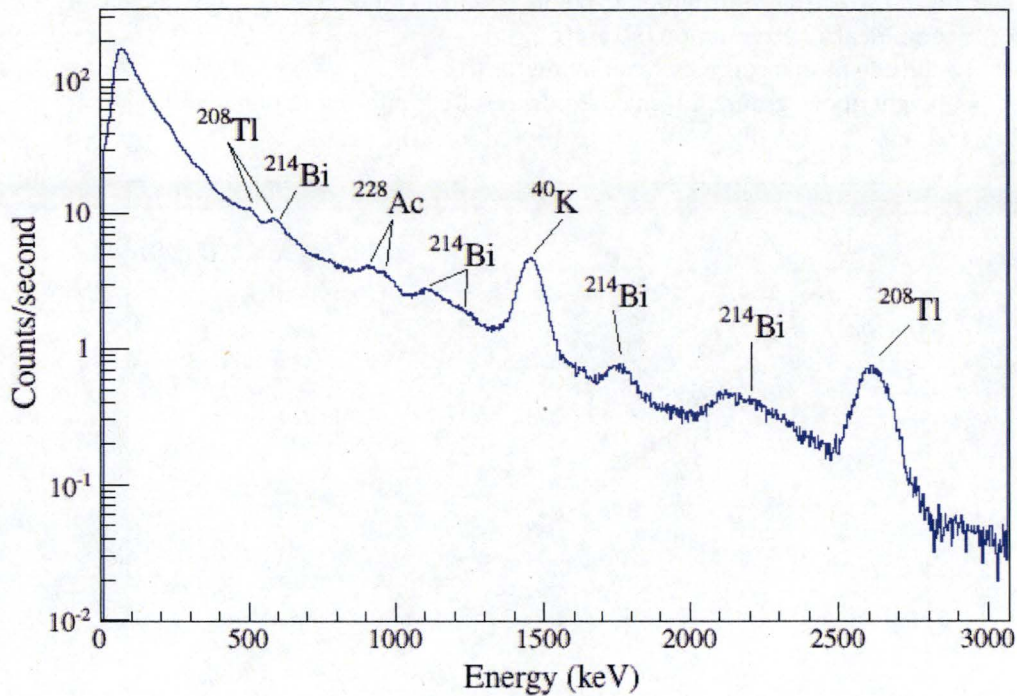


Figure 7: Typical spectrum of natural radioactive background, as measured by the AMS detectors at nominal survey altitude. Annotated peaks are commonly observed signatures of various decay products from radioactive potassium, uranium and thorium.

#### 4.1 Gross Count Rate Analysis and Conversion to Terrestrial Exposure Rate

Gamma rays emanate from many sources, including naturally radioactive uranium, thorium and potassium (and their daughter products) in the earth, airborne radon and radon daughters, and cosmic rays (NCRP 1987). Terrestrial radiation (both from natural and anthropogenic sources) is the quantity of interest for an aerial radiation survey, so the measured count rate is corrected to remove non-terrestrial sources. In order to determine terrestrial radiation levels, gamma-ray count rates due to cosmic rays and airborne radon are subtracted using data collected over the water lines, as described in Section 3.2.

Gamma rays from terrestrial sources interact with and are exponentially attenuated by the air between the ground and the detector at altitude. The attenuation coefficient is determined empirically by collecting data on altitude spiral flights as described in Section 3.2. A series of exponential fits to the data was used to determine the attenuation coefficient ( $\lambda = 0.0017 \pm 0.0001 \text{ ft}^{-1}$ ). One such fit is shown in Figure 8. The inverse exponential attenuation factor is applied to the data at survey altitude to derive the corresponding count rate at the desired height above ground. The net count rate at one meter above ground due only to terrestrial sources is thus calculated by:

$$C_H = (C_G - C_{NT})e^{\lambda(A-H)}$$

where

- $C_H$  = net count rate at height  $H$  above ground due to terrestrial sources (cps),
- $C_G$  = gross count rate measured at survey altitude (cps),

- $C_{NT}$  = non-terrestrial contribution to count rate from radon, cosmic rays, etc. (cps),  
 $\lambda$  = empirical air attenuation factor ( $\text{ft}^{-1}$ ),  
 $A$  = altitude as measured by radar altimeter (ft),  
 $H$  = height above ground at which exposure rate is inferred (1 m = 3.3 ft).

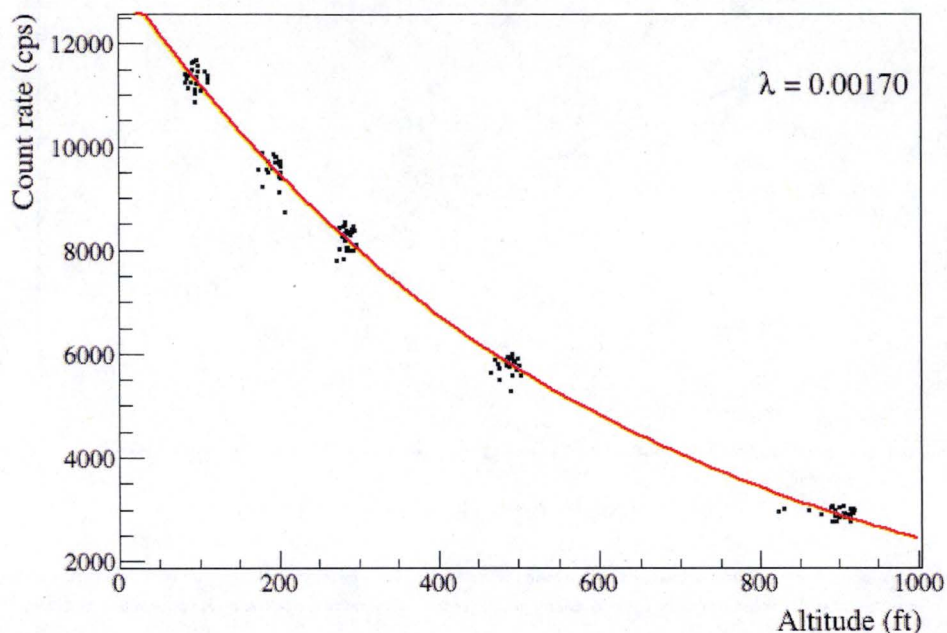


Figure 8: Example fit of altitude spiral flight data. A similar fit was performed on the data from each of three altitude spiral flights to determine the air attenuation coefficient used in this analysis.

The gross count rate  $C_G$  aggregates the count rates from all twelve detectors within a single wide spectral energy window of 21-3000 keV. The non-terrestrial count rate  $C_{NT}$  is determined for each flight from data collected over the water lines. For each individual survey flight, an average count rate from the nearest-neighbor water lines before and after that survey flight were subtracted from the second-by-second gross count rate measurements, as illustrated in Figure 9.

The practical interpretation of  $C_H$  is as a relative measure of gamma radiation due to natural and anthropogenic sources on or in the ground. Further analysis is necessary to convert this to an absolute physical quantity like exposure rate. In general, deriving an exposure rate from gamma ray data involves detailed spectral analysis with some model assumptions that allow conversion of photopeak and Compton-scattered photons to a corresponding exposure. For surveys such as this one involving measurements of small deviations from terrestrial background consisting mostly of naturally occurring radioactive material, an empirical calibration can be performed with aerial data collected over a test line that has also been well-characterized on the ground. The exposure rate due to terrestrial sources then may simply be calculated with the appropriate scaling factor for  $C_H$ ,

$$\dot{X} = \frac{C_H}{F},$$

where  $F$  (cps·h/μR) is the empirically determined conversion factor. For this survey, a conversion factor of  $2950 \pm 240$  cps·h/μR was used, based on data taken in several studies performed by RSL (Colton 1999) (McCullough and Hoteling 2014).

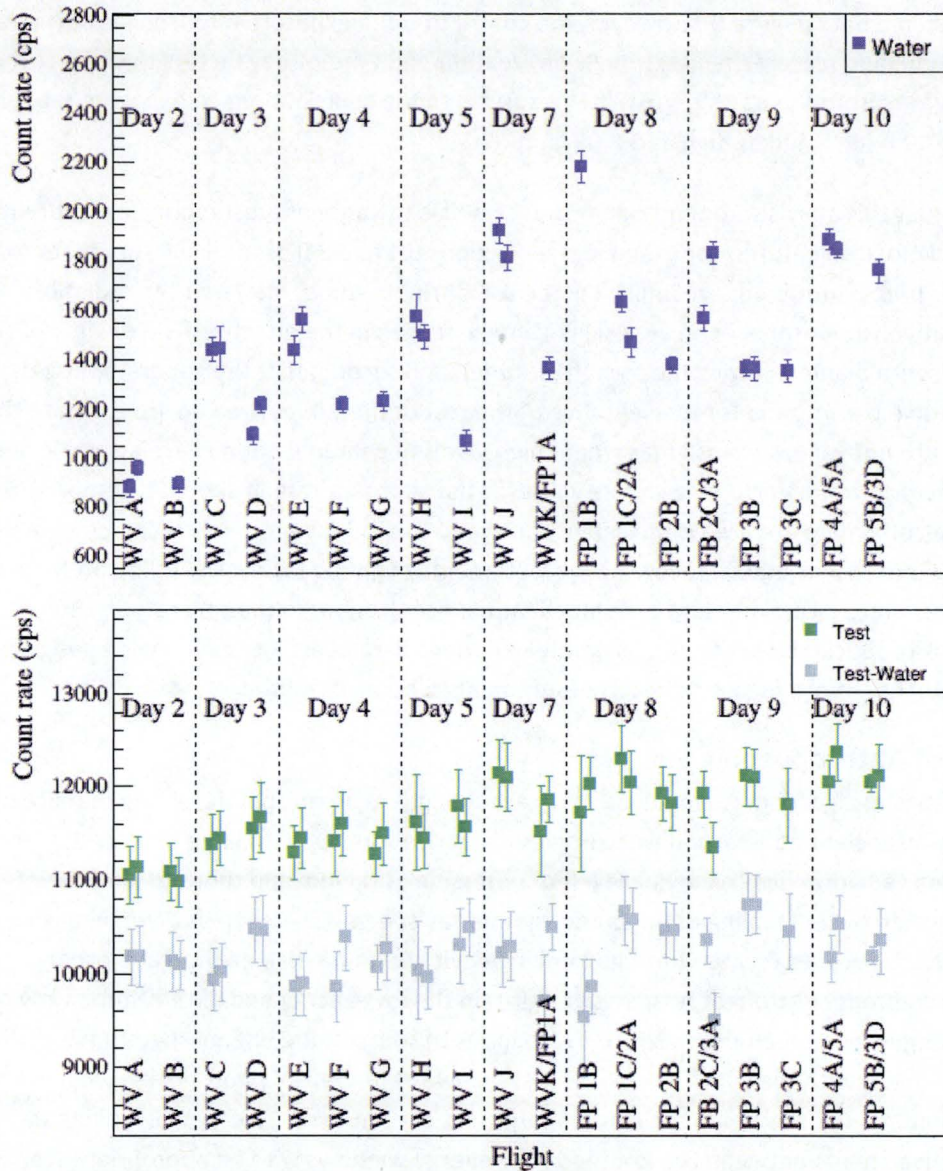


Figure 9: Average count rate over the water line for each survey flight (above), average count rate over the test line both with and without water-line count rate subtraction (below). The water line count rate data were used to remove radon and cosmic-ray contributions to the overall count rate. Note that high-energy (> 3000 keV) cosmic rays which are not included in these count rates contribute significantly to exposure rate. (WV = West Valley flight and FP = Flood Plain flight.)

In order to relate exposure rates from terrestrial sources to total exposure rates, contributions from non-terrestrial sources such as cosmic radiation and airborne radon must be added back to the calculated terrestrial exposure rate. Based on analysis of the current data set using the methodology of

previous studies (McCullough and Hoteling 2014), which also accounts for contributions from higher-energy (> 3000 keV) cosmic-ray photons, the nominal cosmic-ray contribution to the total exposure rate is determined to be  $4.2 \pm 0.1 \mu\text{R/h}$  for this survey, with variations due to local changes in elevation. A value of  $0.6 \mu\text{R/h}$  was chosen as the nominal contribution from airborne radon based on analysis of the water line and test line data (Figure 9). However, the contribution to exposure rate from airborne radon at any particular time and place depends strongly on weather and time-of-day factors that affect the release of radon gases from the earth's crust. In this survey, radon contributions to exposure rate were observed as low as  $0.4 \mu\text{R/h}$  and as high as  $0.8 \mu\text{R/h}$ .

It must be noted that this analysis method can introduce a bias toward underestimating exposure rates for small-scale radiological features; for example, see Sections 6.1 and 8.0 of the 1984 survey report (EG&G/EM 1991). Two assumptions are implicit in the use of this method: first, that the radiation distribution is relatively uniform over an area significantly larger than the effective field of view of the detectors (a circle with diameter twice the aircraft altitude), and second, that the general spectral profile of the test-line background is representative of the rest of the survey area. In areas where these two assumptions are not valid, such as areas where high levels of contamination are relatively localized, this conversion factor may not yield an accurate value for the exposure rate. It should be emphasized, however, that the aerial data are always indicative of radioactivity on the ground and can be reliably used to suggest where more detailed follow-up measurements might be taken. The utility of the aerial data is not as an accurate direct measure of contaminant concentrations in the soil; rather, the interpolative maps produced from the data illustrate variations in radioactivity over a wide geographic area and inform further, more focused direct measurements where warranted.

## **4.2 Analysis of Anthropogenic Sources**

A simple spectral-based algorithm is employed to detect changes in broad spectral shape that are often indicative of the presence of non-naturally occurring radioactive sources. To a large extent, changes in natural background radiation due to varying levels of potassium, uranium and thorium (and their daughters) produce an overall scaling of the broad gamma-ray spectral shape up or down in all energy channels. In contrast, isotopes created through human activity for industrial, medical and other applications tend to produce stronger relative signatures in the low-energy end of the gamma-ray spectrum. To distinguish between the two broad categories of sources, the energy spectrum is divided into two wide windows, with the cutoff energy set just below the 1.46-MeV photopeak from naturally-occurring potassium-40. For this work, the cutoff energy was chosen to be 1365 keV. By taking the difference in relative counts between the low- and high-energy windows with an appropriate scaling factor applied to the high-energy region, a metric to distinguish natural from anthropogenic signatures can be written as

$$C_A = \sum_{E=24}^{1365 \text{ keV}} C(E) - K_A \sum_{E=1365}^{3027 \text{ keV}} C(E),$$

where

$C_A$  = net count rate at survey altitude from anthropogenic sources (cps),  
 $C(E)$  = count rate in the energy channel  $E$  (cps),

and

$$K_A = \frac{\sum_{E=24}^{1365} C_{\text{ref}}(E)}{\sum_{E=1365}^{3027} C_{\text{ref}}(E)}.$$

The ratio  $K_A$  is calculated from data collected over an area known to contain only naturally occurring isotopes (where  $C_{\text{ref}}(E)$  is the count rate in the energy channel  $E$  for data taken in this reference area), and therefore represents the expected ratio of low-to-high-energy counts in the spectrum due to natural terrestrial background. The difference  $C_A$  thus measures deviation from an expected spectral shape due to natural sources. Note that this metric will fluctuate about zero for normal variations in the spectral signature from naturally occurring radioactive material. Interpolated contour maps of the  $C_A$  metric are useful for identifying areas where more detailed spectral analysis should be performed or more detailed ground measurements should be taken to determine specific isotopic content.

### 4.3 Isotopic Extractions

Extraction of radiation signatures from specific isotopes on the ground follows an analogous procedure to the anthropogenic source analysis, but with more selectively and precisely chosen spectral windows. A three-window method was employed in this work to infer a net count rate representing the relative contribution to the data from an isotope of interest. In this case the isotope of interest is cesium-137, which remains on and in the ground as a long-lived contaminant in areas around the WNYNSC.

The three-window isotopic extraction is calculated with the expression

$$C_{3W} = \sum_{E_3}^{E_4} C(E) - K_3 \left[ \sum_{E_1}^{E_2} C(E) + \sum_{E_5}^{E_6} C(E) \right],$$

where

$C_{3W}$  = net count rate at survey altitude from isotope of interest (cps),  
 $C(E)$  = count rate in the energy channel  $E$  (cps),  
 $[E_3, E_4]$  = energies bounding the photopeak window (keV),  
 $[E_1, E_2], [E_5, E_6]$  = energies bounding the low-energy and high-energy background windows, respectively (keV),

and

$$K_3 = \frac{\sum_{E_3}^{E_4} C_{\text{ref}}(E)}{\sum_{E_1}^{E_2} C_{\text{ref}}(E) + \sum_{E_5}^{E_6} C_{\text{ref}}(E)},$$

with  $C_{\text{ref}}$  defined as for the anthropogenic extraction algorithm. In the absence of any photopeak signature of the isotope of interest, this metric will fluctuate about zero.

For this work, the energy windows for cesium-137 extraction were chosen as follows:

$$\begin{aligned} [E_1, E_2] &= [522, 591] \text{ keV,} \\ [E_3, E_4] &= [636, 696] \text{ keV,} \\ [E_5, E_6] &= [738, 807] \text{ keV.} \end{aligned}$$

An illustration of the cesium-137 extraction method is shown in Figure 10 for both strong and weak cesium-137 spectral signatures. Note that the lower-energy background window is chosen to minimize interference from the 609-keV spectral line from naturally occurring bismuth-214 (from the uranium-238 decay chain).

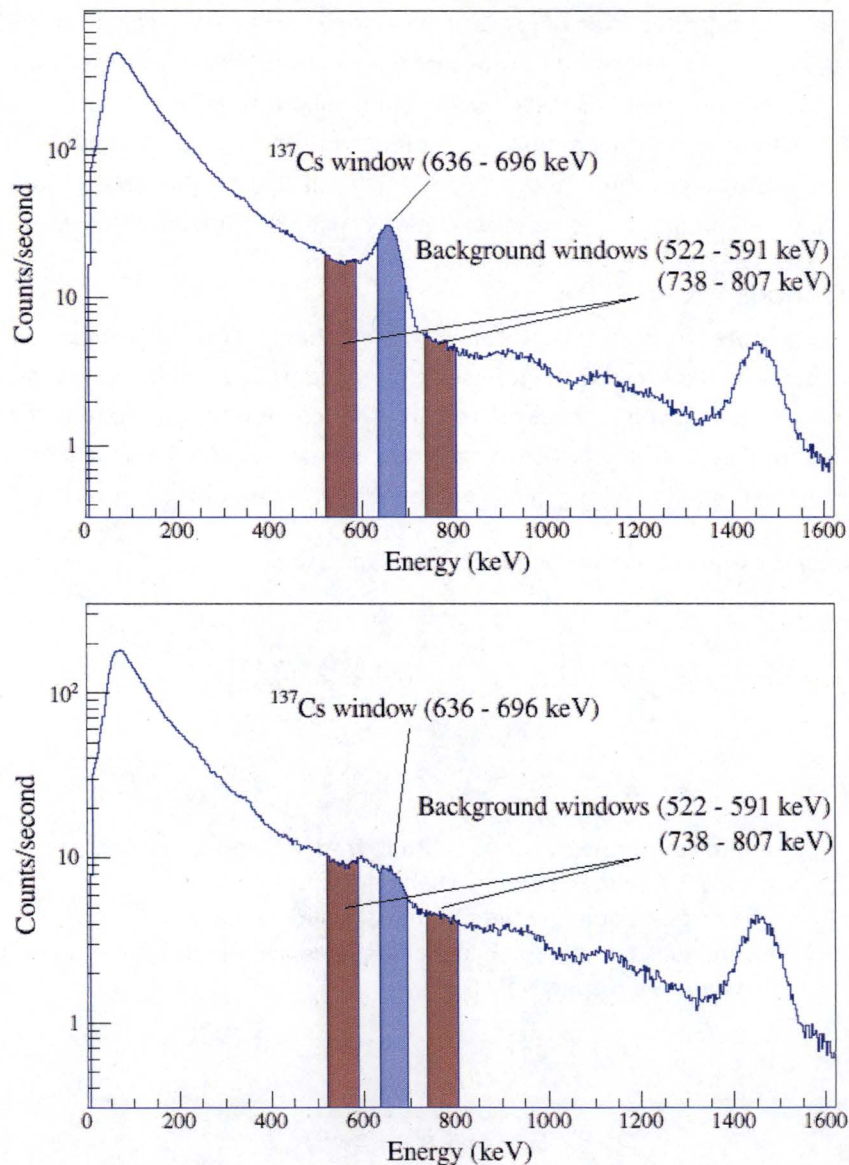


Figure 10: Three-window isotopic extraction from spectrum with strong (above) and weak (below) Cs-137 signatures.

Within the boundaries of the WVDP, an area of radioactive waste storage on the north side of the site exhibited a strong spectral signature of cobalt-60. A two-window spectral extraction was performed on

the entire data set for cobalt-60 and the isotopic signature was seen to be completely localized to the on-site storage area (see Section 0). The two-window algorithm is similar to the anthropogenic extraction algorithm described in Section 0, except that the low-energy window is set to encompass the pair of cobalt-60 photopeaks at 1173 keV and 1332 keV ( $[E_1, E_2] = [1128 \text{ keV}, 1380 \text{ keV}]$ ) and the high-energy window is set around a wide "background" area where no cobalt-60 signature, including Compton-scattered gamma rays, would appear in the spectrum ( $[E_3, E_4] = [1449 \text{ keV}, 3000 \text{ keV}]$ ). The scaling factor  $K$  is calculated with the analogous ratio of photopeak-window to background-window count rates.

## **5 Survey Results**

### **5.1 Fixed Ground Measurements**

Several "ground truth" measurements were collected to provide verification for the exposure rate conversion factor used in this work and to provide a closer look at some areas of particular interest in the survey area. These measurements were carried out with the three instruments described in Section 3.1. The discussion presented in this section will focus primarily on the PIC measurements and direct comparisons to the aerial measurement results. Figure 11 and Figure 12 show the 25 PIC measurement locations taken within the aerial survey area and measured exposure rates overlaid on the interpolated exposure rate maps calculated from the aerial data. In these figures, the exposure rate as measured by the PIC has been corrected to exclude contributions from radon and cosmic rays to facilitate direct comparison to the aerial data. PIC measurements taken along the test line and at the AMS base of operations fall outside of the aerial survey area and are not shown on the maps presented here. The interpolated exposure rate maps will be discussed in Section 5.2.

The ground measurements were carried out in five general regions: along the test line, along the altitude spiral, within the boundaries of the WVDP ("site interior"), outside the boundaries of the WVDP but within WNYNSC territory ("site exterior"), and within the Cattaraugus Creek flood plain survey boxes ("flood plain"). The first two regions were specifically selected as areas that appeared to be relatively uniform in terrain so that the radiological signature would not vary significantly over the field of view of the aerial system. Hence, these data provide a good test for the accuracy of the exposure rate conversion factor utilized in this work. In contrast, measurements collected from the site interior are expected to contain significant contributions from materials that are housed, stored, and buried at the facility. In this case, rather large discrepancies are expected to be present between the ground and aerial measurements owing to the difference in the exact field of view between the two methodologies. Finally, the site exterior and flood plain measurements provide spot checks at various positions within the survey area that may or may not represent good cases for comparison between the two methodologies.

Comparisons with the aerial data presented here were obtained by extracting the exposure rate value from the interpolated exposure rate contour determined from the AMS measurements and adding the contribution from cosmic rays. This was done at the coordinates of each of the ground measurements.

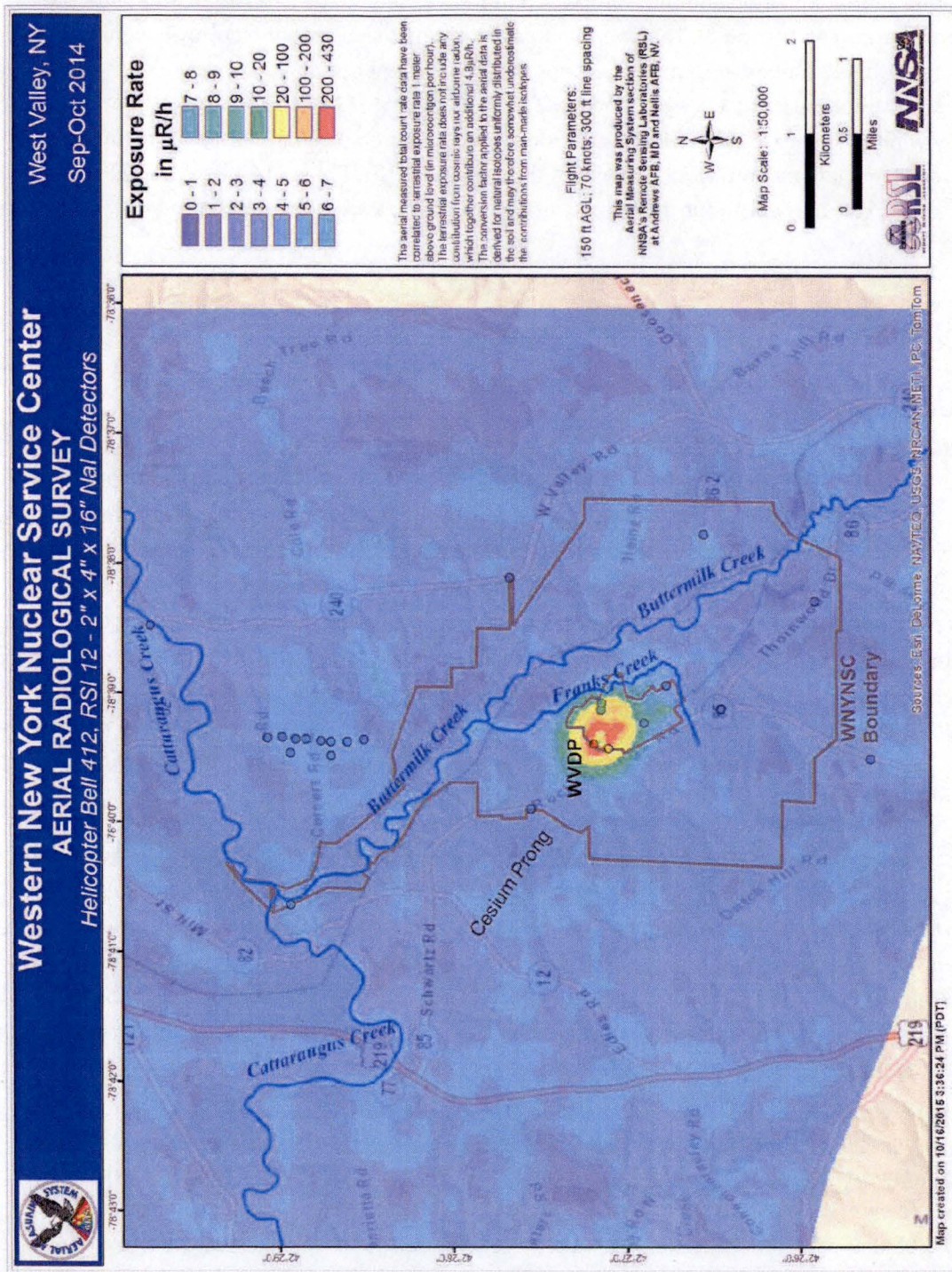
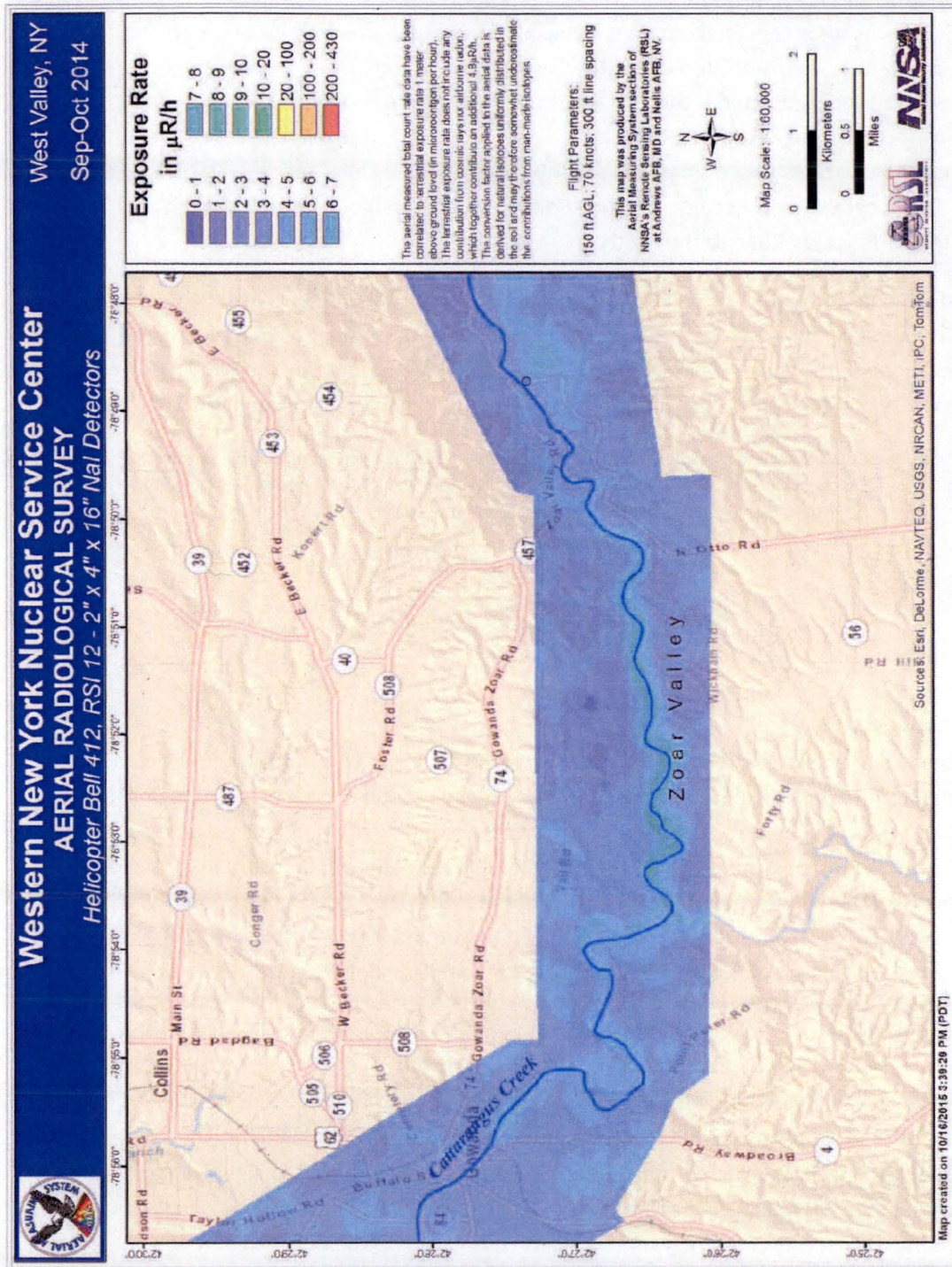


Figure 11: Exposure rate measurements (circles) taken with the pressurized ionization chamber on and around the WNYNSC, overlaid on the inferred terrestrial exposure rate map from aerial survey data. PIC exposure rates have been corrected to eliminate contributions from radon and cosmic rays to facilitate direct comparison to the aerial data. (The location of the "cesium prong" is annotated here for consistency with the anthropogenic and isotopic extraction maps presented later in this report.)



### 5.1.1 Test Line and Altitude Spiral

Five measurements were collected on the test line alongside Thiel Langford Road (Route 249) between Ketchum Road (Route 494) and Eden Road. The average results from these measurements are listed in Table 1. Here, the value depicted is the average from all of the measurements, with an uncertainty representing the standard deviation of those data points. Similarly, the average results from six measurements along the altitude spiral line are listed in this table, along with the associated standard deviation. Those data were collected alongside Bond Road and bounded by a 90-degree turn in the road to the north and Emerson Road to the south.

The individual measurements for the test line and altitude spiral data are displayed in the top panel of Figure 13 as a direct comparison between the AMS-extracted value and the PIC result. Good agreement is observed between the values extracted from aerial data and measured by the PIC, largely within the total uncertainty of 8.5% in the exposure rate calculation (McCullough and Hoteling 2014).

Table 1: Comparison of average exposure rates for measurements carried out on the test line, altitude spiral, and site exterior. Error bars indicate the standard deviation of the measurements conducted within these regions. These reported exposure rates include the contributions from airborne radon and cosmic rays as well as terrestrial sources.

Measurement	AMS ( $\mu\text{R/h}$ )	PIC ( $\mu\text{R/h}$ )
Test Line	$9.2 \pm 0.1$	$9.3 \pm 0.1$
Altitude Spiral	$9.1 \pm 0.2$	$8.9 \pm 0.3$
Site Exterior	$8.7 \pm 0.4$	$8.9 \pm 0.3$

### 5.1.2 Site Interior

Measurements were collected at seven locations inside the WVDP site boundary; however, as noted above, the difference in field of view between the aerial and ground measurement systems led to significant disagreement in the results. Additionally, if the gamma radiation field emanating from one of the WVDP facilities were asymmetrically shielded, it would result in a larger estimate of the exposure rate from aerial data than from ground data. In most cases the value determined from the aerial data was significantly higher than that measured by the PIC. A summary of the results from these measurements is displayed on a logarithmic scale in the middle panel of Figure 13.

Of particular interest in this region is a measurement along Rock Springs Road located within the so-called "cesium prong," an area contaminated by an uncontrolled release in 1968 (USDOE/NYSERDA 2010). Neither the aerial nor PIC measurements show particularly high exposure rate values at this point ( $8.5 \mu\text{R/h}$  and  $8.8 \mu\text{R/h}$ , respectively). However, it should be noted that the high-resolution gamma-ray spectral data in this area indicate cesium-137 activity. The isotopic extraction algorithm applied to the aerial data yields similar results, indicating the presence of cesium-137 in this area. Qualitatively, the levels of cesium-137 seen in spectra from the cesium prong area exceed the levels seen in other survey areas (well outside of the cesium prong) where similar exposure rates were observed. This implies that exposure rate alone is not a reliable measure of cesium-137 contamination.

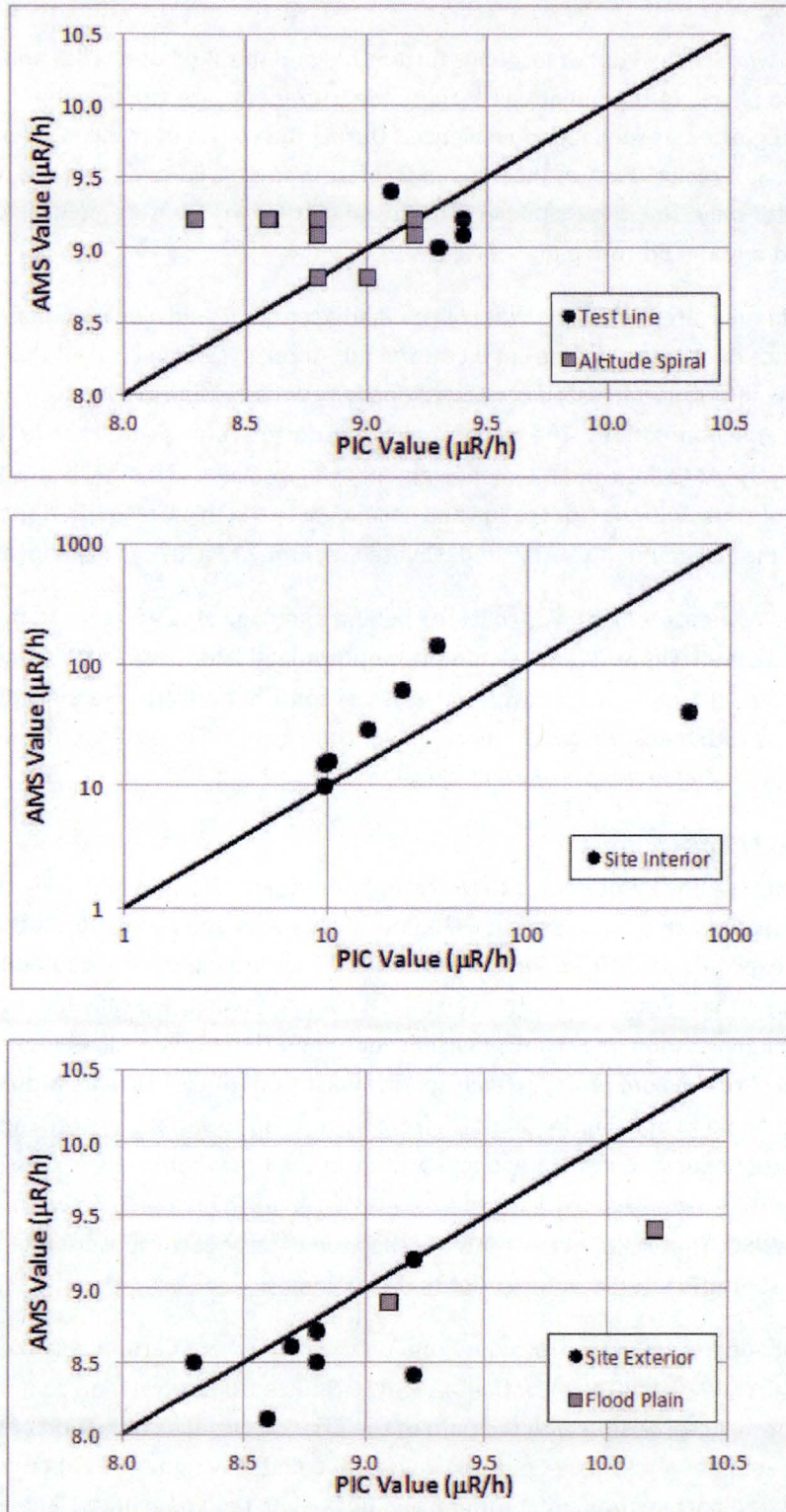


Figure 13: Comparison of exposure rates from AMS and PIC measurements. The top panel shows results for test line and altitude spiral, the middle panel shows results for site interior measurements, and the bottom panel shows results for the site exterior and flood plain. The straight lines indicate a perfect correlation, added as a guide for the eye. Note the logarithmic axes in the middle plot.

### **5.1.3 Flood Plain**

Several measurements were carried out at locations further beyond the site boundaries and along the Cattaraugus Creek flood plains. (Although not all of these measurements are strictly within the flood plain area, they are categorized as such for convenience.) During the course of these measurements, the PIC malfunctioned and, as a result, most of the flood plain measurements were carried out with the gamma-ray spectrometer only. The discussion here is focused on the two measurements in which the PIC was used, as depicted in the bottom panel of Figure 13.

Of these two flood plain measurements, one was collected adjacent to a field along Thomas Corners Road near the confluence of Buttermilk Creek and Cattaraugus Creek (visible in Figure 11). This area was selected for measurement because elevated cesium-137 activity was seen in a preliminary analysis of the aerial data during survey operations. The results indicate exposure rates slightly above those in neighboring areas, with the AMS data and PIC measurements giving values of 9.4  $\mu\text{R}/\text{h}$  and 10.2  $\mu\text{R}/\text{h}$ , respectively (inclusive of contributions from radon and cosmic rays). The high-resolution spectrum taken in parallel with the PIC measurement also indicated elevated cesium-137 activity at this location.

The second flood plain PIC measurement was collected behind a parking area adjacent to the Otto Road bridge over Cattaraugus Creek (Figure 12). Exposure rates determined from AMS and PIC data at this location were 8.9  $\mu\text{R}/\text{h}$  and 9.1  $\mu\text{R}/\text{h}$ , respectively (inclusive of contributions from radon and cosmic rays), which is consistent with measurements collected over the neighboring regions. The high-resolution spectra did not indicate the presence of elevated Cs-137 levels.

## **5.2 Exposure Rate Maps**

Exposure rate at one meter above ground due to terrestrial sources was determined using the method in Section 4.1, and the interpolated maps are shown below in Figure 14 and Figure 15. As the figures illustrate, background exposure rates from terrestrial sources where no radioactive contamination would be expected (other than global fallout from historical nuclear testing) typically fall within the range 2-5  $\mu\text{R}/\text{h}$  (not including radon and cosmic-ray contributions). There is very slight visual evidence in the exposure rate map of the cesium prong extending northwest from the WVDP site. More pronounced, but comparable in magnitude (6-8  $\mu\text{R}/\text{h}$  from terrestrial) to variations seen throughout the survey area is the elevated exposure rate extending north from the site where Frank's Creek flows into Buttermilk Creek. Relatively strong exposure rates in excess of 100  $\mu\text{R}/\text{h}$  are confined well within the boundaries of the WNYNSC. The "hole" in the center of the area of strongest exposure rate above the WVDP arises from the saturation of the detectors at that location.

There is also an area of apparent elevated exposure rate on the map where Cattaraugus Creek flows east-to-west in the Zoar Valley area. The elevation is slight (6-8  $\mu\text{R}/\text{h}$  from terrestrial) compared to background, but it is strongly correlated with the path of the Creek. Careful examination of the spectral data taken above that area of Cattaraugus Creek, however, revealed only signatures of the natural terrestrial background: radioactive uranium, thorium, and potassium (and daughters). The elevation in exposure rate is most likely due to the geography of that area, where the Creek flows through a gorge with steep slopes on both sides. While the AMS helicopter maintains its nominal survey altitude over the creek bed directly below, the raised terrain on either side of the aircraft contributes significantly to the

gamma-ray count rate in the detectors. Implicit in the application of the exposure rate algorithm is that terrestrial radiation contributions within the detectors' field of view come from a relatively flat geometry; when this assumption is poor (e.g., flying over a gorge or canyon), the estimated exposure rate may be inaccurate and must be interpreted carefully. A similar effect was observed in an "urban canyon" setting during a recent survey of Boston, Massachusetts (Hoteling, McCullough and Beal 2014).

All other areas of the exposure rate map are consistent with expected normal variations in natural background.

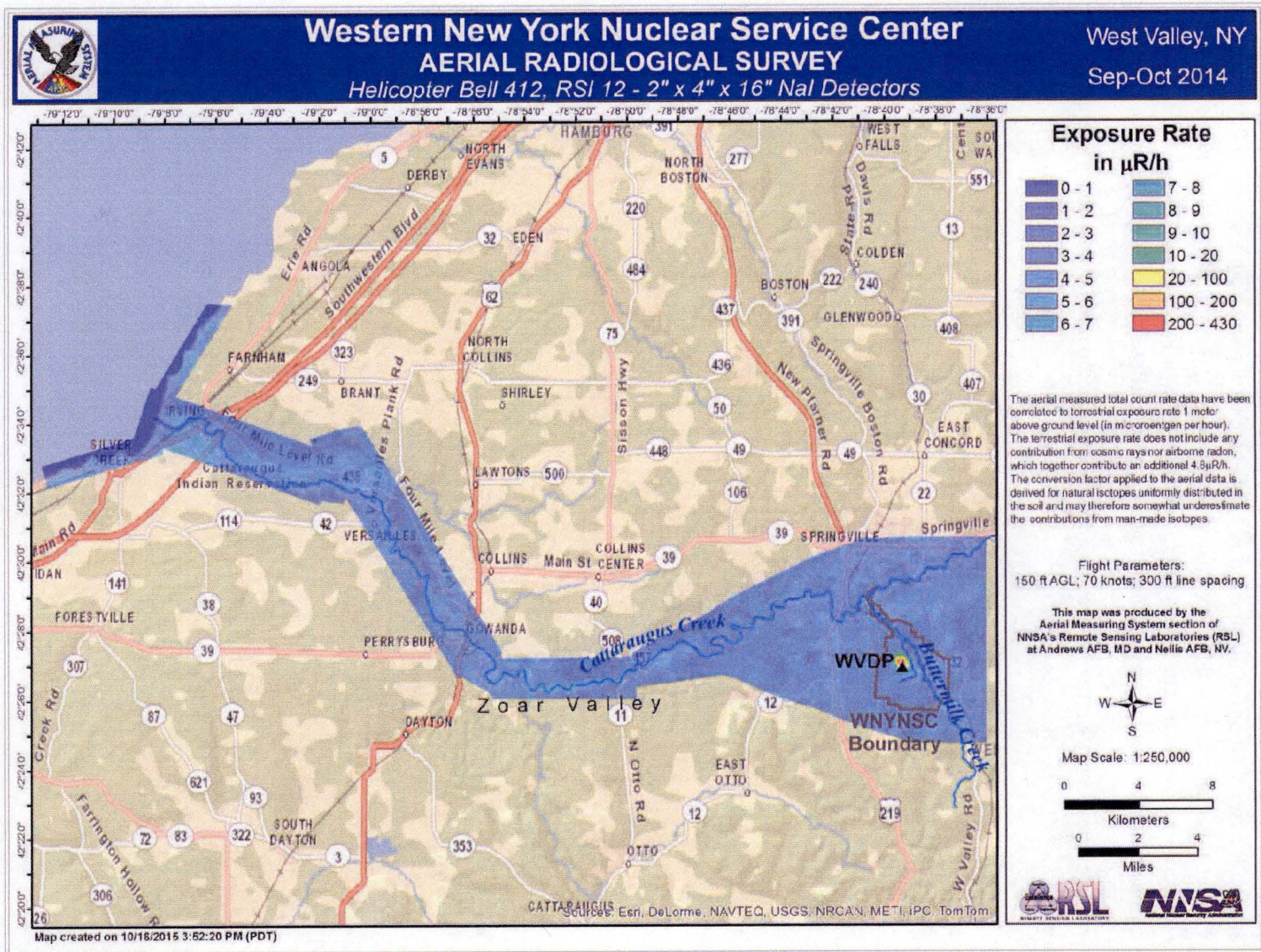


Figure 14: Map of inferred exposure rates at 1 m above ground due to terrestrial sources (full survey area).

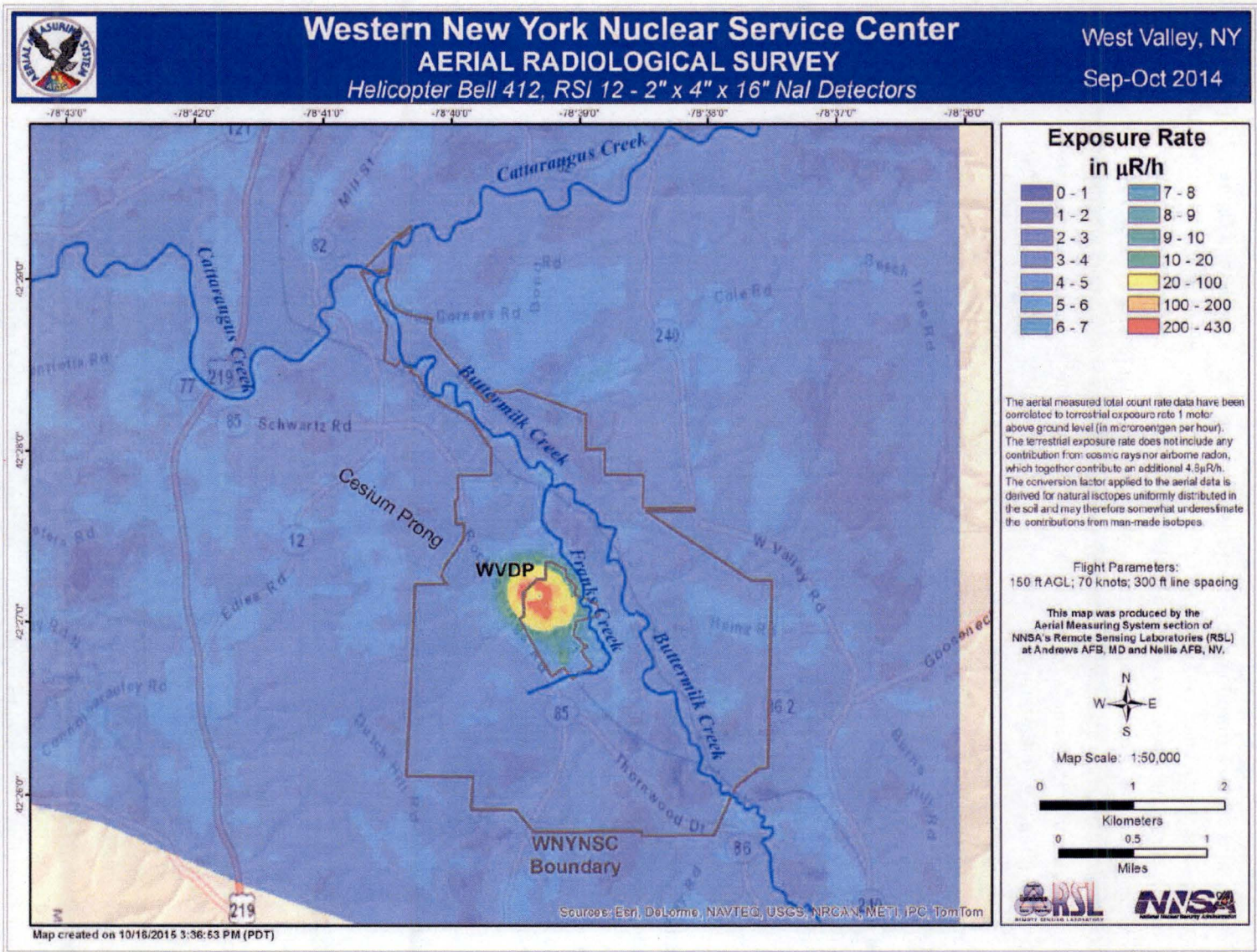


Figure 15: Map of inferred exposure rate at 1 m above ground due to terrestrial sources (detail over WNYNSC). The location of the "cesium prong" is annotated here for consistency with the anthropogenic and isotopic extraction maps presented later in this report.

### **5.3 Anthropogenic Extractions**

Interpolated results of the anthropogenic extractions are mapped in Figure 16 and Figure 17. The reference area used to calculate the scaling factor  $K_A$  is an approximately circular area with 3500' radius located roughly three miles southeast of the WVDP, in the extreme southeastern corner of the survey area. (The same area was used to calculate the analogous scaling factors for the cesium-137 and cobalt-60 isotopic extraction algorithms.) The cesium prong is quite evident here where it was not so in the exposure rate map. The same is true of the parallel prong to the northeast that follows Buttermilk Creek to its confluence with Cattaraugus Creek. This is expected, because although low levels of cesium-137 deposition may not contribute much to the exposure rate on the ground, the anthropogenic extraction algorithm is designed to be sensitive to radioisotopes with low-energy gamma-ray signatures below 1365 keV (cesium-137 emits 662-keV gamma rays).

Elevated count rates are again observed in the Zoar Valley region of Cattaraugus Creek, this time in the anthropogenic extractions. As stated in the discussion of derived exposure rates above, spectral signatures from this elevated area indicate only naturally occurring radioisotopes. Although the anthropogenic extraction algorithm is designed to suppress variations in natural background, it is based on the assumption that the ratio of counts between the low- and high-energy regions of the spectrum is approximately constant for natural sources. For non-flat terrestrial features where gamma rays are scattered differently, this is a poor assumption, and the Zoar Valley features appear in the extractions as elevated relative count rates.

Southeast of Scoby Hill Dam (labeled in Figure 17), in a region north of Schwartz Road and on both sides of US Route 219, are a couple of areas of elevated relative count rates (1000-2000 counts per second, or approximately 2-4 standard deviations above background) in the anthropogenic extractions. These areas do not appear to correlate with the path of the creek or with any other particular geographic feature. Investigation of the spectra from aerial data shows an excess of cesium relative to background at levels comparable to those seen in parts of the cesium prong outside the WNYNSC and in parts of Buttermilk Creek north of the WVDP.

In the southeast corner of the Flood Plain 3 survey box (approximate coordinates  $42^{\circ} 32.5'$  latitude,  $-79^{\circ} 2.5'$  longitude), in a wooded area south of Four Mile Level Road, there is another area of elevated relative count rates (1000-2000 counts per second, or approximately 2-4 standard deviations above background). Investigation of the spectrum (Figure 18) reveals a very slight excess of cesium relative to background. This area will be discussed further in Section 5.4.

Throughout the rest of the survey area, there are other small spots of slightly elevated count rates in the anthropogenic extractions. The spectral signatures from these areas have all been thoroughly investigated for evidence of cesium-137 and other non-naturally occurring isotopes, and except for an isolated radiopharmaceutical signature (see Section 5.4.3), none were found. The anthropogenic extraction algorithm is sensitive to statistical fluctuations in the high-energy count rate even when only naturally occurring isotopes are present.



Figure 16: Interpolated map of count rates due to non-naturally occurring sources, as determined from the anthropogenic extraction algorithm (full survey area).

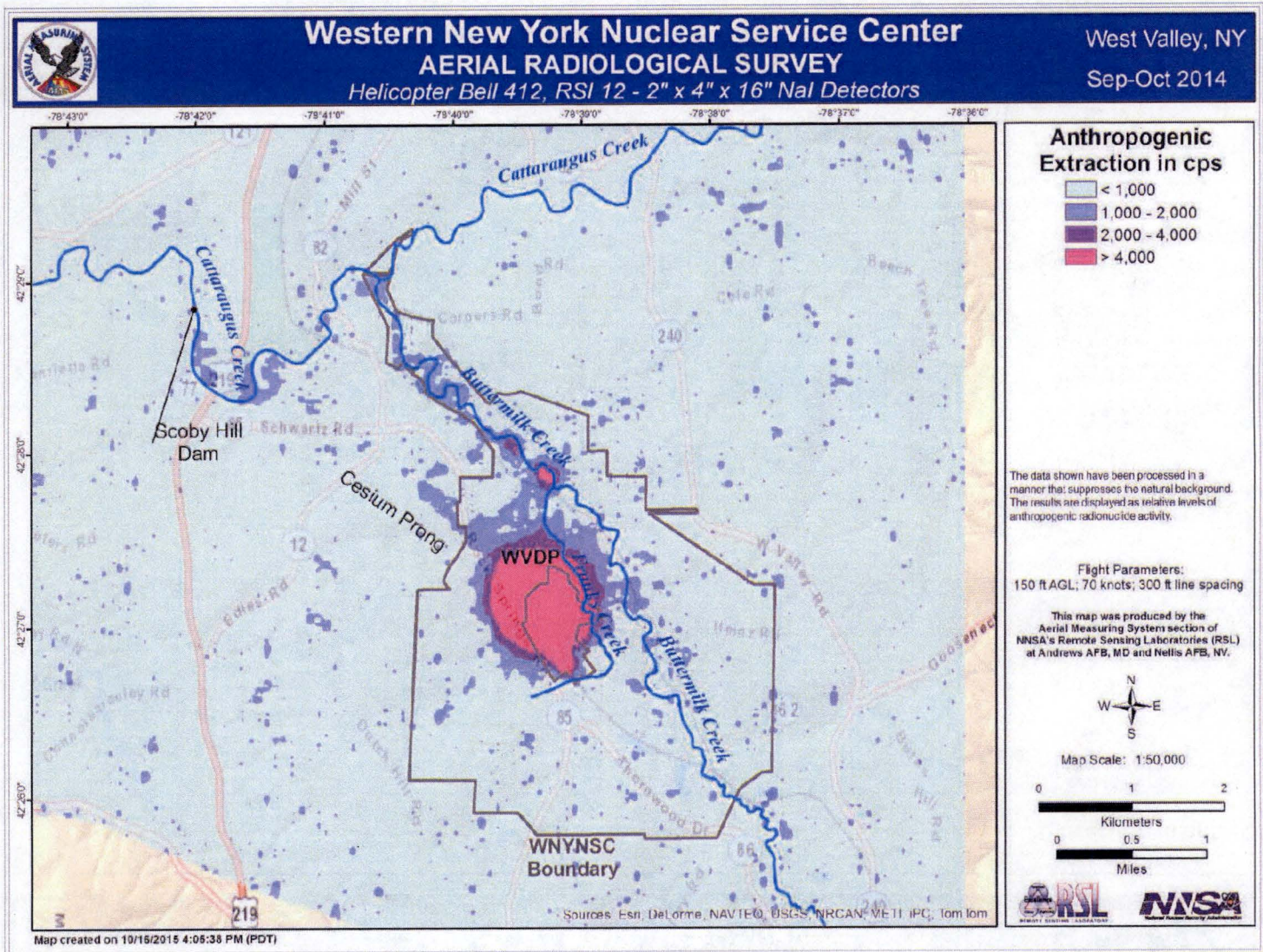


Figure 17: Interpolated map of count rates due to non-naturally occurring sources, as determined from the anthropogenic extraction algorithm (detail over WNYNSC).

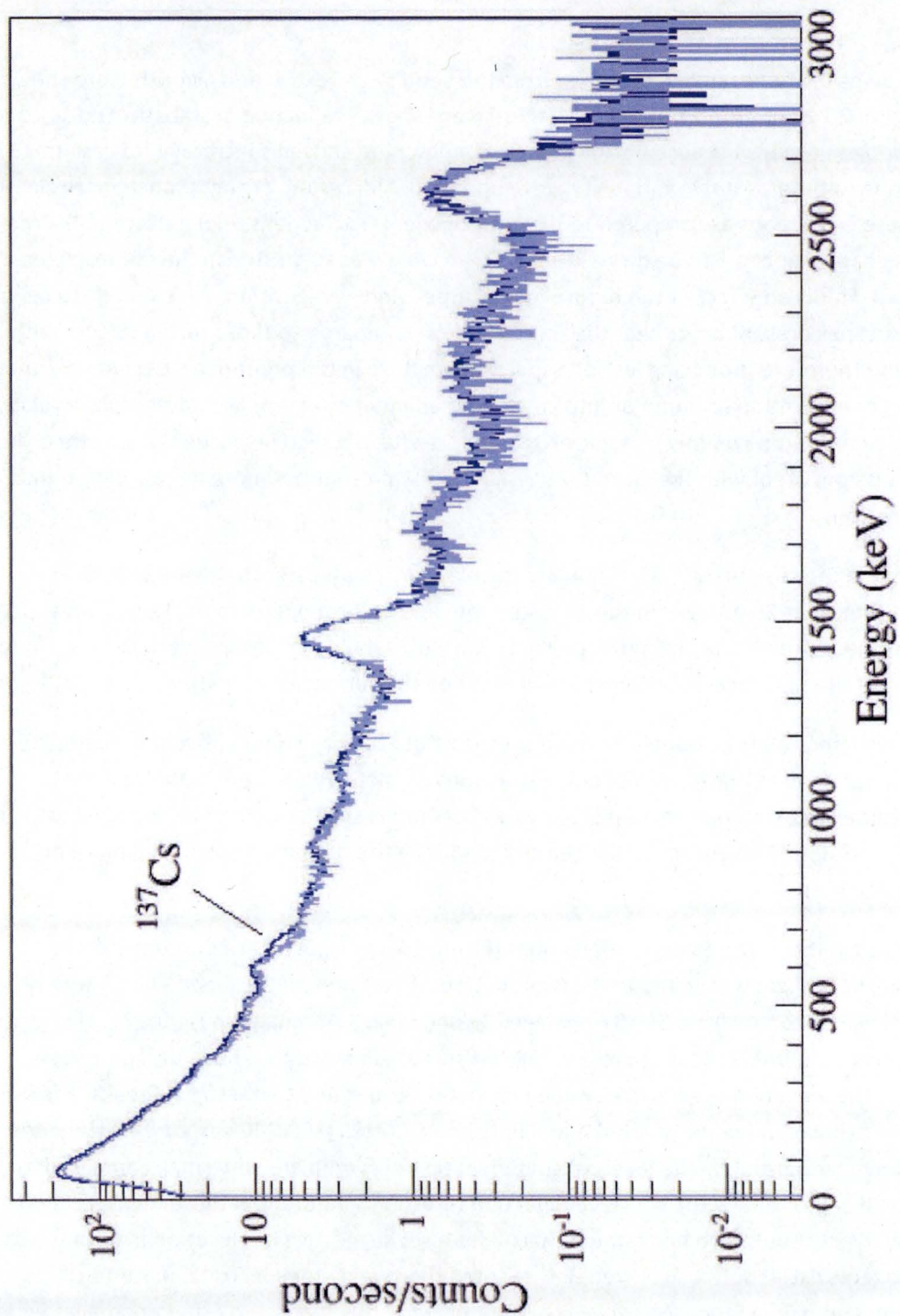


Figure 18: Slight signature of cesium-137 relative to background (light blue) in the aggregate spectrum (dark blue) of aerial data taken over the area of elevated count rates in the southeast corner of the Flood Plain 3 survey box. This signature was evident in both the anthropogenic extractions and in the cesium-137 isotopic extractions.

## **5.4 Isotopic Extractions**

### **5.4.1 Cesium-137**

Interpolated maps of count rates determined from the cesium-137 extraction algorithm are shown in Figure 19, Figure 20 and Figure 21. In general, these maps show a reduction in statistical noise compared to the anthropogenic maps because narrow energy windows are chosen specifically for cesium-137 and fluctuations due to other isotopic variability are suppressed. The cesium prong is much more clearly defined in these extractions as compared to the anthropogenic extractions. Along Buttermilk Creek, the cesium-137 signature appears to be more localized than what was suggested in the anthropogenic extraction map. This is an effect of the nature of the three-window algorithm, which tends to be more sensitive to isotopes present on or near the soil surface, as compared to those mixed deeper within the soil column and therefore producing less of a spectral signature in the photopeak. Cesium-137 that has migrated deeper into the soil column or into creek bed sediment over time would produce a relatively weaker signal in the three-window isotopic extraction. Careful, detailed inspection of spectra collected over this area is consistent with the claim that cesium-137 is present but more deeply buried than in neighboring regions.

Notably absent in the cesium-137 extraction are the elevated count rates that were seen over Cattaraugus Creek near Zoar Valley in the exposure rate and anthropogenic extractions. This supports the claim that these are effects of topography only. Careful, detailed inspection of these spectra reveals no indications of the presence of cesium-137 (whether on the surface or buried).

The areas of elevated relative counts observed southeast of Scoby Hill Dam (labeled in Figure 20) and north of Schwartz Road in the anthropogenic extractions are not evident here in the cesium-137 extraction, although as stated in Section 5.3, levels of cesium in slight excess of background were seen in the aerial spectral data. This suggests that the cesium-137 in this area might be mixed more deeply within the soil column.

As was observed in the anthropogenic extractions (Figure 16 and Figure 17), count rates from cesium-137 are very slightly elevated in the identified southeast area of the Flood Plain 3 survey box. This area of elevated counts from Cs-137 is labeled "Flood Plain 3 Anomaly" in Figure 21. The relative count rate elevation (30-60 cps, or approximately 2-4 standard deviations above background) is comparable to the elevation seen at the confluence of Buttermilk and Cattaraugus Creeks, and less than what was seen at the confluence of Frank's and Buttermilk Creeks (120-240 cps, or 8-16 standard deviations above background). The levels of contamination observed are very small compared to background and lie just above the sensitive detection thresholds inherent in these measurement and analysis methods. It should also be restated that all features suggestive of elevation in both the isotopic and anthropogenic extraction results were investigated thoroughly for spectral signatures of contamination, and beyond the cases specifically identified in this report, no other anomalies were observed.

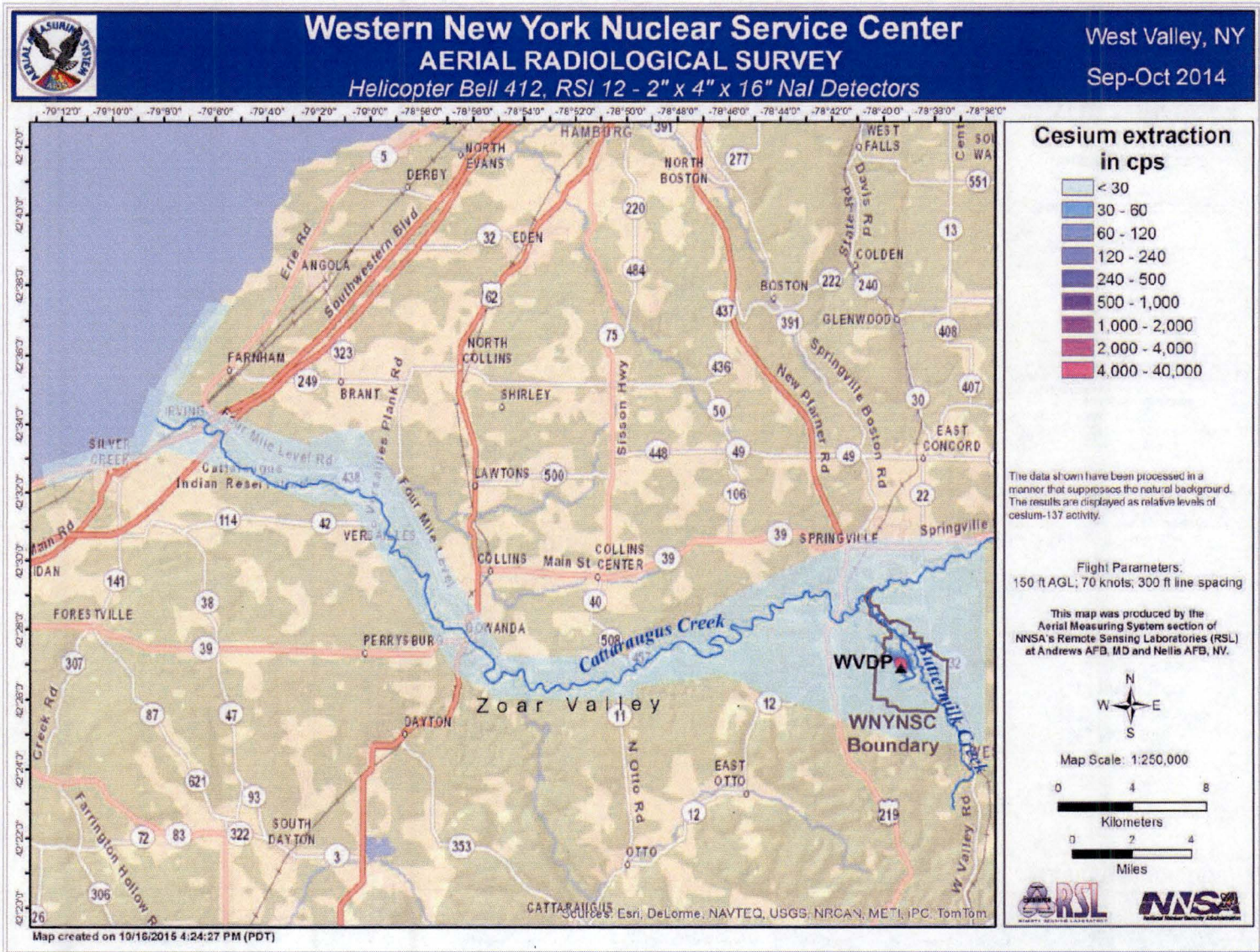


Figure 19: Interpolated map of count rates from cesium-137 isotopic extraction (full survey area).

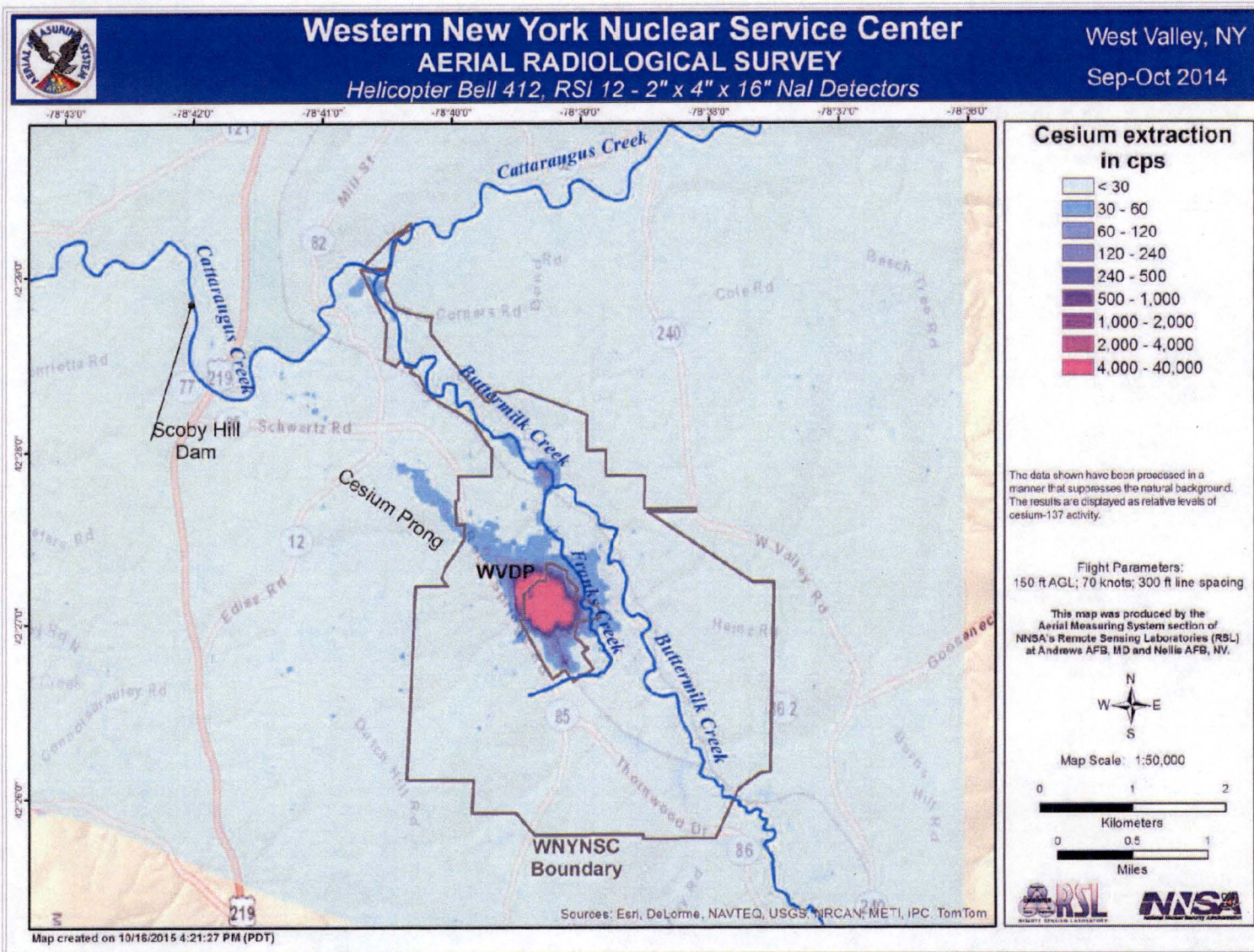


Figure 20: Interpolated map of count rates from cesium-137 isotopic extraction (detail over WNYNSC).

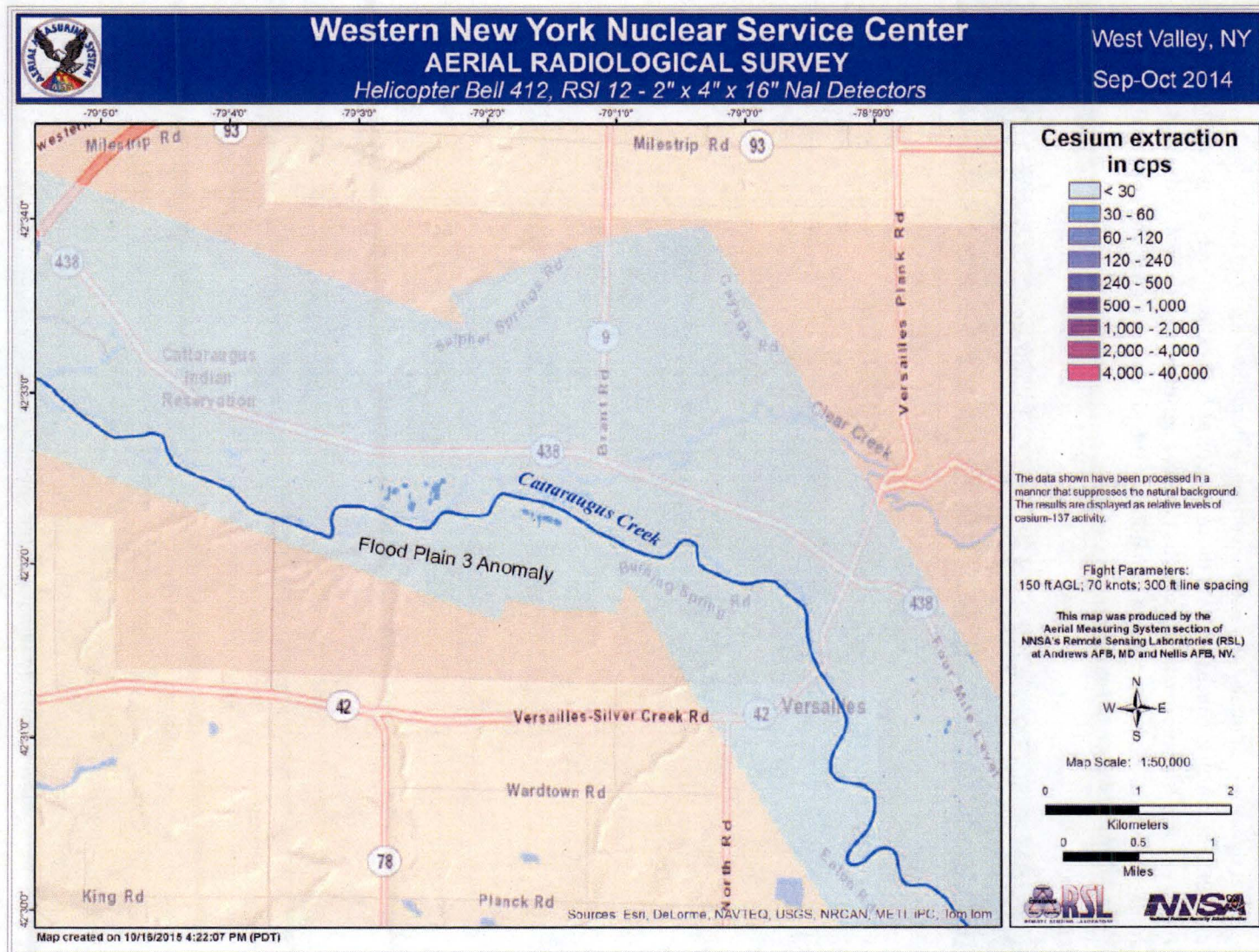


Figure 21: Interpolated map of count rates from cesium-137 isotopic extraction (detail over western Cattaraugus Creek). The area of elevated count rates from Cs-137 south of Four Mile Level Road is indicated as "Flood Plain 3 Anomaly."

### 5.4.2 Cobalt-60

A strong spectral signature of cobalt-60 was observed while flying over a pair of structures on the north side of the WVDP site, which is consistent with those structures being known radioactive waste storage facilities. A two-window isotopic extraction of cobalt-60 was performed on the entire data set and only the area around the waste storage exhibited signatures of the isotope. A map of the cobalt-60 extraction over WVDP is shown in Figure 22.

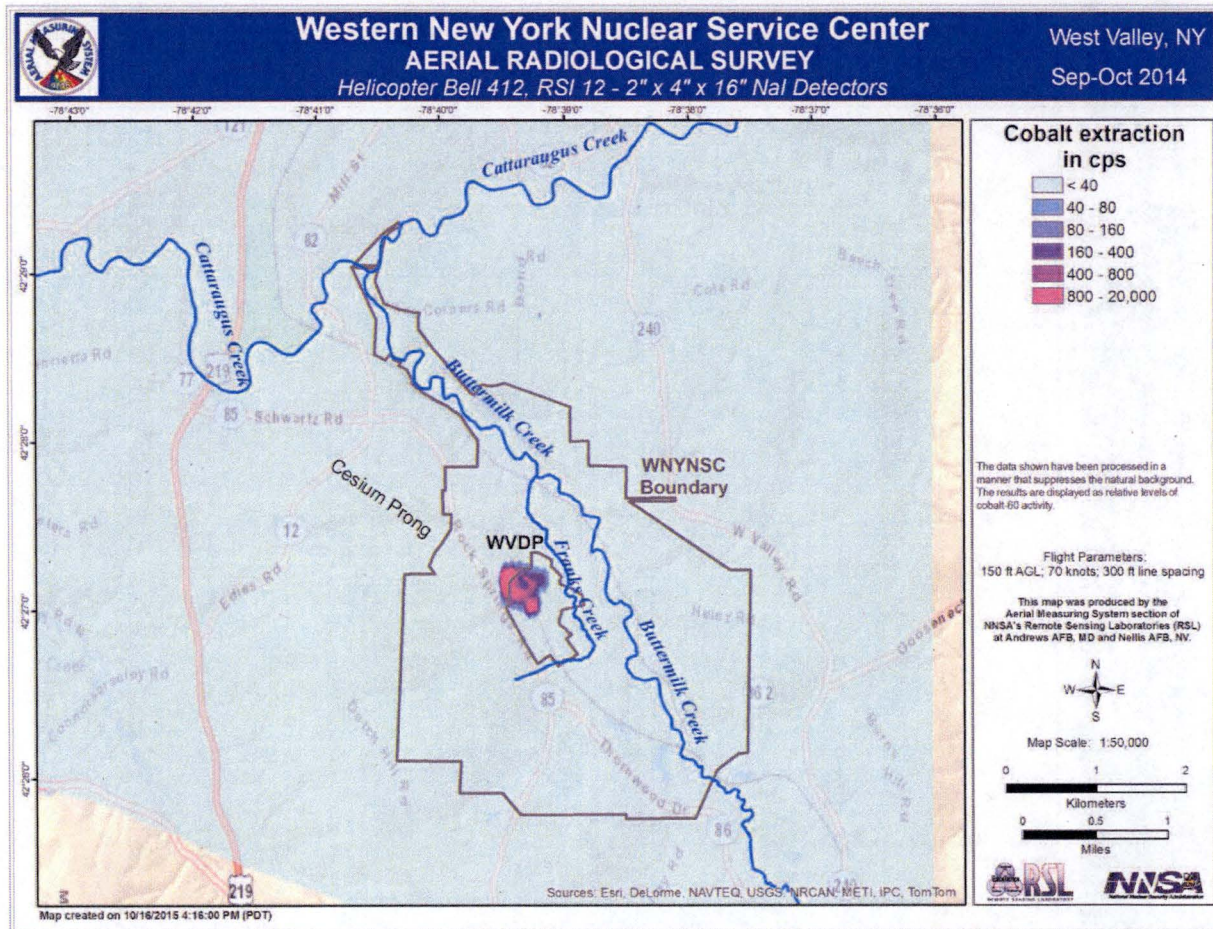


Figure 22: Interpolated map of count rates from cobalt-60 isotopic extraction (detail over WNYNSC). Cobalt-60 signatures were not observed anywhere else in the survey area.

### 5.4.3 Technetium-99m

No other significant spectral signatures were seen in the data to prompt another isotopic extraction on the entire data set. However, one additional isolated spectral feature was observed, which was analyzed and identified as technetium-99m, a radiopharmaceutical commonly used in diagnostic imaging. The isotope was seen in four seconds of spectral data collected over a building between Four Mile Level Road and Thomas Indian School Drive in Irving, New York (approximate location 42° 32.34' latitude, -78° 59.75' longitude). The signature was identifiable as technetium-99m with a high level of

confidence from the 141-keV peak in the spectrum (Figure 23). Radiopharmaceuticals such as technetium-99m are frequently observed during radiological surveys of populated areas and are usually attributable to a person who has undergone a recent medical procedure or to a medical facility where such procedures are performed.

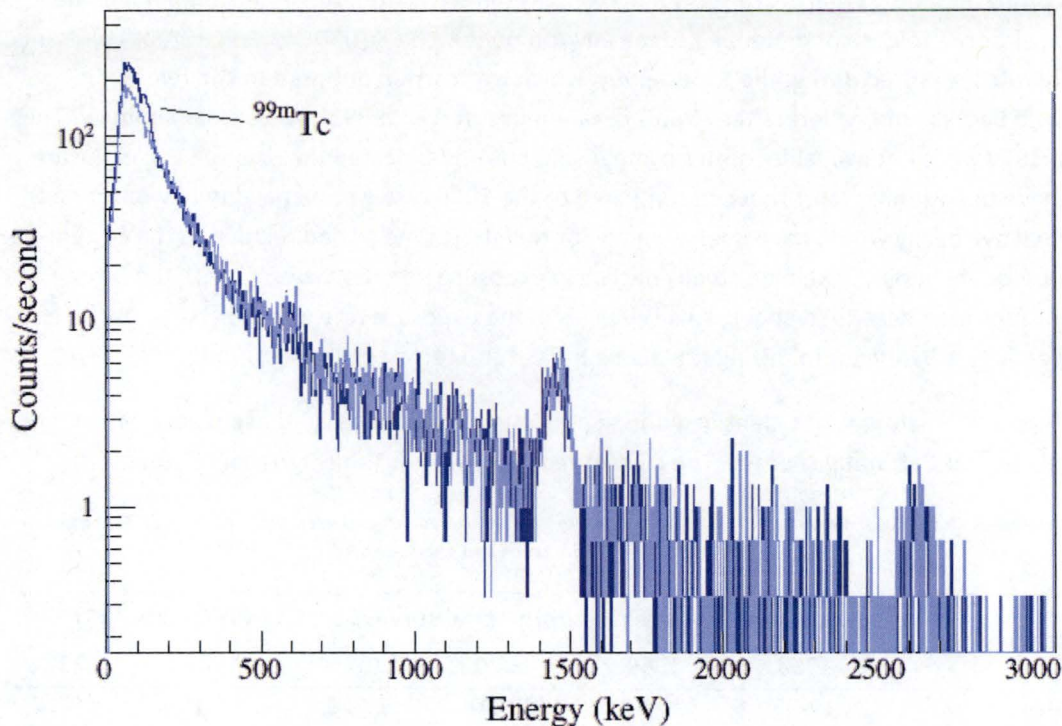


Figure 23: Signature of technetium-99m relative to background (light blue) in the aggregate spectrum (dark blue) of aerial data taken over Irving, New York near Thomas Indian School Drive. The common radiopharmaceutical is identified by the peak at 141 keV.

## 5.5 Comparison to Previous Surveys

### 5.5.1 Representative Exposure Rates from Selected Areas

Table 2 lists ranges of representative exposure rates (including radon and cosmic-ray contributions) at selected areas of interest from several aerial surveys conducted over and around the WVDP site between 1968 and 2014, which is modified and updated from a similar table presented in the report from the 1979 survey (EG&G/EM 1981). As stated in Section 5.2, background exposure rates from terrestrial sources where no radioactive contamination would be expected typically fall within the range 2-5  $\mu\text{R/h}$  (not including radon and cosmic-ray contributions). To understand the results presented in Table 2, it must be noted that reprocessing activities at the plant were terminated in 1972. Thus, the measured exposure rate at Frank's and Buttermilk Creeks exhibit an increase in magnitude from 1968 to 1970, followed by a steady decline from 1970 to present. This decline in exposure rate comes from a combination of radioactive decay (the half-life for cesium-137 is 30.2 years) and weathering effects. Cattaraugus Creek, which is further downstream than the others, showed a slight increase in exposure rate from 1968 to 1969, and the exposure rate appears to have remained fairly steady, if not slightly

lower, in subsequent surveys. This apparent difference in behavior over time is likely a consequence of the fact that the cesium-137 activity there was initially much lower, so that analogous effects from radioactive decay and weathering are simply more difficult to discern from the ubiquitous background signature.

The cesium prong area near Quarry Creek is fundamentally different from the others in that it came from a single airborne release of material into the environment in 1968 (USDOE/NYSERDA 2010). Hence, the exposure rate measured during the 1968 survey, which was carried out prior to the release, is consistent with background, whereas the exposure rate measured in 1969 shows a clear anomaly. The results from 1970 were not available for this comparison, but it is expected that the spike in exposure rate would have been similar to or reduced compared to the 1969 result primarily due to weathering effects (radioactive decay would have been minimal for this short time period relative to the cesium-137 half-life). Subsequent surveys exhibit a steady decline in exposure rate; however, as with the Cattaraugus Creek area described above, small changes in the exposure rate due to varying low levels of cesium-137 activity are difficult to distinguish above the natural terrestrial background.

The Flood Plain 3 anomaly was not identified during previous surveys because those measurements did not cover this area of Cattaraugus Creek. The current result is listed in Table 2 for completeness.

Table 2: Exposure rate at ground level measured at various areas of interest from aerial surveys between 1968 and present. These exposure rates include contributions from radon and cosmic rays.

Region	Measured exposure rate from aerial surveys around WVDP site ( $\mu\text{R/h}$ )					
	1968	1969	1970	1979	1984	2014
Frank's Creek	15-25	20-50	30-70	17-22	11-15	8-14
Buttermilk Creek	< 15	15	15-30	9-22	11-25	8-12
Cattaraugus Creek	15	20	15	10-14	11-13	8-10
Cesium prong <sup>1</sup>	5-10	20-25		9-13	11-13	8-12
Flood Plain 3 anomaly						8-9

<sup>1</sup> The cesium prong was previously referred to as the Quarry Creek Anomaly (Barasch and Beers 1971).

### 5.5.2 Comparison of Current Results to 1984 Survey

Exposure rates and anthropogenic and isotopic extractions from the aerial survey data taken in 1984 over the WNYNSC (EG&G/EM 1991) have been reprocessed with current software and mapped for comparison with the 2014 survey. These maps are presented in Figure 24. On the exposure rate maps, the color scales are identical, facilitating a direct visual comparison between absolute quantities. The extracted anthropogenic and isotopic count rates, on the other hand, depend on the type of algorithm used (two-window versus three-window), the chosen parameters (selection of energy windows), and the efficiency of the detection system, and therefore cannot be directly compared as calculated. To accommodate comparison, the color scales on the corresponding anthropogenic and cesium-137 extraction maps have been chosen so that similar colors indicate the same relative elevations compared to background, in terms of the number of standard deviations above background. In the anthropogenic extractions, for example, the blue color indicates a range of 600-1200 counts per second in the 1984

map and 1200-2400 counts per second in the 2014 map, but in both cases represents 2-4 standard deviations above background. In this way the survey results can be compared directly.

Comparison of the exposure rate maps (Figure 24, top row) shows that, in general, elevated exposure rates seen in the 1984 data along the cesium prong and along Frank's and Buttermilk Creeks are approaching levels close to background in the 2014 data, consistent with the trends noted in Table 2. The footprint of high exposure rates on the WVDP site has shifted to the northwest end of the site, although the apparent extent of the high exposure rates may be an artifact of the spatial averaging effect of aerial measurements, as described in Sections 4.1 and 5.1.2. Note that the 1984 data exhibit a higher overall background exposure rate than the 2014 data by about 2-3  $\mu\text{R}/\text{h}$ ; however, the reduction in exposure rates along Buttermilk and Cattaraugus Creeks from 1984 to 2014 exceeds what could be explained by this simple baseline shift in the data and is likely due to radioactive decay and weathering. The systematic 2-3  $\mu\text{R}/\text{h}$  downward shift in background exposure rate levels from 1984 to 2014 may be an artifact of gross differences in technology and subtle differences in choice of analytical parameters between the two surveys. The previous survey was conducted over thirty years ago with different hardware and software, and with a different body of prior work from which to draw in determining exposure rate conversion factors.

From the anthropogenic and cesium-137 maps (Figure 24, middle and bottom rows), it is observed on the south side of the WVDP site that the 1984 survey data exhibit a double-lobed feature in both extractions, with the stronger signature arising from the eastern lobe. In the 2014 data, the elevated eastern lobe has disappeared, consistent with the northwestern shift observed in the exposure rate footprint between 1984 and 2014.

In the 1984 anthropogenic and cesium-137 extraction data, there was also a "filament" of elevated count rates along Frank's Creek leading into Buttermilk Creek. This feature has significantly weakened in the current data set. In the cesium-137 extraction, for example, the 1984 map shows elevations as high as 16 standard deviations above background levels, whereas in the 2014 data, the same region is only 2-4 standard deviations above background. Analysis of the spectra in the 2014 data from that region does reveal a cesium-137 signature, so it has not completely disappeared, but its levels are significantly reduced. The weakening of the Frank's Creek filament is representative of the trend in the cesium-137 maps from 1984 to 2014 as a whole; it is clear that the cesium prong, the elevated area at the confluence of Buttermilk and Cattaraugus Creeks, and all other offsite features have significantly weakened in the past thirty years. This is likely due to a combination of radioactive decay and weathering effects that distribute and disperse radioactive materials from the surface soil.

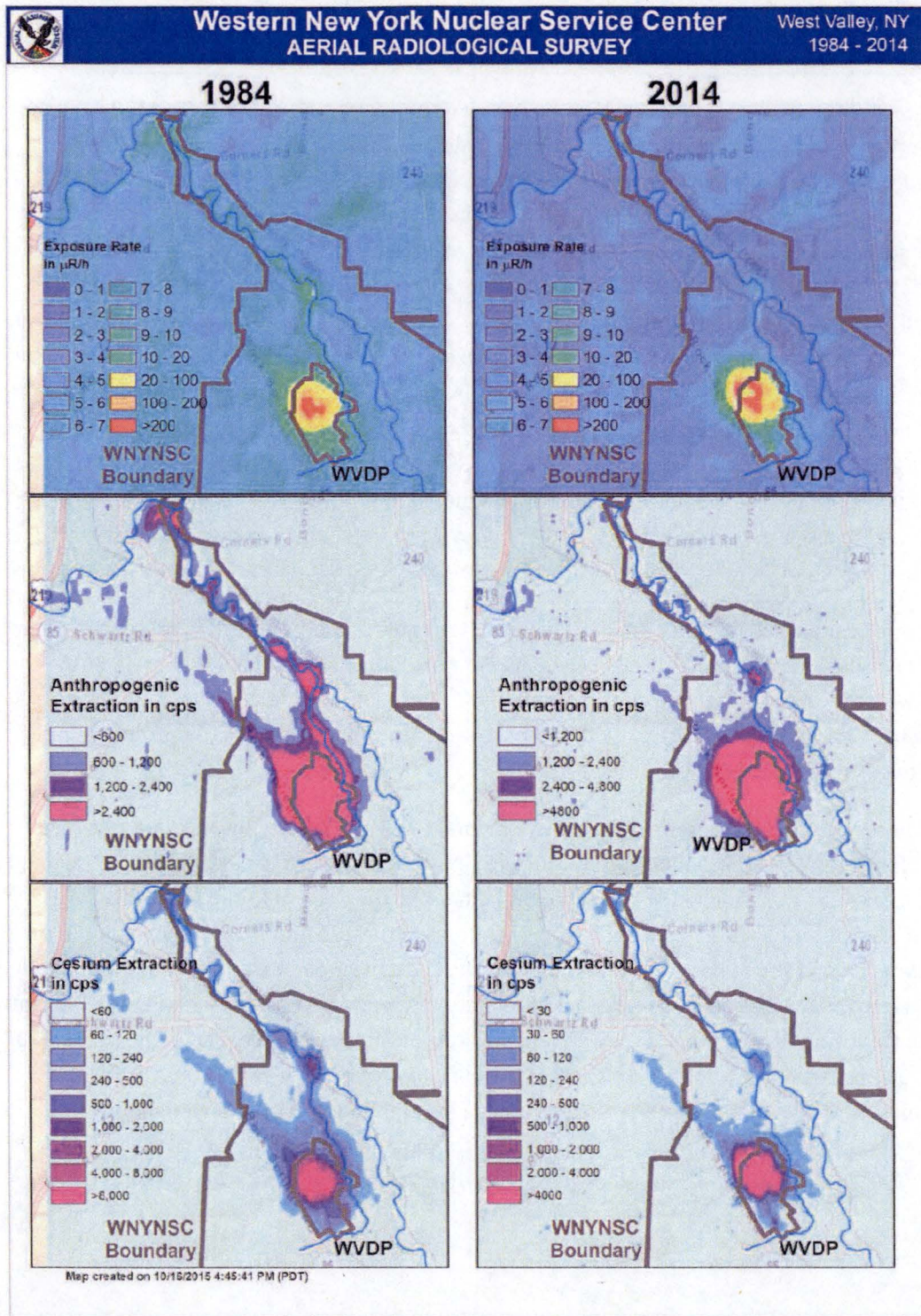


Figure 24: Comparison of the 2014 survey to the 1984 survey. For the exposure rate maps (top row), the color maps are identical and may be compared directly. Threshold values in the color maps for the anthropogenic (middle row) and cesium-137 (bottom row) extractions are chosen such that similar colors correspond to the same elevations relative to background (number of standard deviations above background), and may also be directly compared.

## References

- Barasch, G. E., and R. H. Beers. *Aerial Radiological Measuring Surveys of the Nuclear Fuel Services Plant, West Valley, New York, 1968 and 1969 (EGG 1183-2235)*. EG&G, 1971.
- Colton, D.P., Hendricks, T.J. *Radiological Characterization of the Lake Mohave Test Line (DOE/NV/11718-024)*. Las Vegas, NV: Bechtel Nevada, 1999.
- EG&G/EM. *A comparison of Aerial Radiological Survey Results of the Nuclear Fuels Services Center (NFS) and Surrounding Area (EP-F 001)*. EG&G/EM, 1981.
- EG&G/EM. *An Aerial Radiological Survey of the West Valley Demonstration Project and Surrounding Area (EGG-10617-1080)*. EG&G/EM, 1991.
- Hoteling, N. J., T. L. McCullough, and W. C. Beal. *Aerial Radiological Survey of the Boston Marathon Race Route (Draft report)*. RSL internal report, 2014.
- McCullough, T. L., and N. J. Hoteling. *Determination of Exposure Rate Conversion Coefficient for Aerial Measurement System Application*. RSL internal report, 2014.
- NCRP. *Exposure of the Population in the United States and Canada from Natural Background Radiation (Report No. 94)*. Washington, DC: NCRP, 1987.
- Proctor, A. E. *Aerial Radiological Surveys (DOE/NV/11718-127)*. Las Vegas, NV: Bechtel Nevada, 1997.
- USDOE/NYSERDA. *Final Environmental Impact Statement for Decommissioning and/or Long-Term Stewardship at the West Valley Demonstration Project and Western New York Nuclear Service Center (DOE/EIS-0226)*. West Valley, NY: USDOE/NYSERDA, 2010.

## **Survey Parameters**

Survey Site:	Western New York Nuclear Service Center and Cattaraugus Creek in western New York
Survey Coverage:	Approximately 90 square miles (233 km <sup>2</sup> )
Survey Dates:	September 22 – October 4, 2014
Survey Aircraft:	Bell 412 Helicopter
Nominal Survey Altitude:	150 feet (46 meters)
Nominal Aircraft Speed:	70 knots (36 meters per second)
Line Spacing:	300 feet (91 meters)
Navigation System:	Trimble differential GPS receiver (WAAS corrections)
Detector Configuration:	Twelve 2" x 4" x 16" NaI(Tl) detectors (four RSI RSX-3 units)
Acquisition System:	One RSI RS-501 and four RS-701 units
Exposure Rate Conversion Factor:	2950 ± 240 cps-h/μR
Air Attenuation Coefficient:	0.0017 ± 0.0001 ft <sup>-1</sup>
Survey Team:	
AMS Mission Manager:	Bill Beal
Pilots:	Alex Brid, Grant Ebner, Tim Rourke, Michael Toland
Equipment Technologists:	Kevin Borders, Michael Lukens, Jason Moore, Tom Stampahar
Data Analysts:	Ashlee Dailey, Jezabel Stampahar
Mission Scientists:	Sarah Bender, Nathan Hoteling, Russell Malchow, Michael Mazur, Piotr Wasiolek
Aircraft Mechanics:	Katie Hildermann, Ed Zachman